Blind CSI Acquisition for Multi-Antenna Interference Mitigation in 5G Networks

by

©Ali AbdulMawgood Ali Ali Esswie

A Dissertation submitted to the School of Graduate Studies in partial fulfillment of the requirements for the degree of

Master of Computer Engineering

Faculty of Engineering and Applied Science

Memorial University of Newfoundland

October 2017

St. John's Newfoundland

Abstract

Future wireless communication networks are required to satisfy the increasing demands of traffic and capacity. The upcoming fifth generation (5G) of the cellular technology is expected to meet 1000 times the capacity that of the current fourth generation (4G). These tight specifications introduce a new set of research challenges. However, interference has always been the bottleneck in cellular communications. Thus, towards the vision of the 5G, massive multi-input multi-output (mMIMO) and interference alignment (IA) are key transmission technologies to fulfil the future requirements, by controlling the residual interference.

By equipping the base-station (BS) with a large number of transmit antennas, e.g, tens of hundreds of antennas, a mMIMO system can theoretically achieve significant capacity with limited interference, where many user equipment (UEs) can be served simultaneously at the same time and frequency resources. A mMIMO offers great spatial degrees of freedom (DoFs), which boost the total network capacity without increasing transmission power or bandwidth. However, the majority of the recent mMIMO investigations are based on theoretical channels with independent and identically distributed (i.i.d) Gaussian distribution, which facilitates the computation of closed-form rate expressions. Nonetheless, practical channels are not spatially uncorrelated, where the BS receives different power ratios across different spatial directions between the same transmitting and receiving antennas. Thus, it is important to

understand the behavior of such new technology with practical channel modeling.

Alternatively, IA is known to break the bottleneck between the capacity of the network and the overall spectral efficiency (SE), where a performance degradation is observed at a certain level of connected user capacity, due to the overwhelming inter-user interference. Theoretically, IA guarantees a linear relationship between half of the overall network SE and the online capacity by aligning interference from all transmitters inside one spatial signal subspace, leaving the other subspace for desired transmission. However, IA has tight feasibility conditions in practice including high precision channel state information at transmitter (CSIT), which leads to severe feedback overhead.

In this thesis, high-precision blind CSIT algorithms are developed under different transmission technologies. We first consider the CSIT acquisition problem in MIMO IA systems. Proposed spatial channel estimation for MIMO-IA systems (SCEIA) shows great offered spatial degrees of freedom which contributes to approaching the performance of the perfect-CSIT case, without the requirements of channel quantization or user feedback overhead. In massive MIMO setups, proposed CSIT strategy offered scalable performance with the number of the transmit antennas. The effect of the non-stationary channel characteristics, which appears with very large antenna arrays, is minimized due to the effective scanning precision of the proposed strategy. Finally, we extend the system model to the full dimensional space, where users are distributed across the two dimensions of the cell space (azimuthal/elevation). Proposed directional spatial channel estimation (D-SCE) scans the 3D cell space and effectively attains additional CSIT and beamforming gains. In all cases, a list of comparisons with state-of-the-art schemes from academia and industry is performed to show the performance improvement of the proposed CSIT strategies.

To the soul of my mother...

Acknowledgements

I would like to express my sincere thanks and deepest gratitude to my supervisors Dr. Octavia A. Dobre and Dr. Salama Ikki for the wonderful opportunity they granted me. Their valuable supervision, guidance, and dedication have all pushed me beyond my expectations.

I would like to acknowledge my received financial support, provided by Dr. Dobre and Dr. Ikki, School of Graduate Studies at Memorial University, and the Natural Sciences and Engineering Research Council of Canada (NSERC), Discovery program.

I would like to thank all the academic staff in the Electrical and Computer Engineering Department, along with my group members who provided me with valuable assistance on both technical and personal levels.

Table of Contents

List of Tables

List of Figures

List of Abbreviations

IoE	internet of everything
5G	fifth generation
4G	fourth generation
IA	interference alignment
mMIMO	massive multi-input multi-output
BS	base-station
UE	user equipment
DoFs	degrees of freedom
i.i.d	independent and identically distributed
SE	spectral efficiency
CSIT	channel state information at transmitter
FDD	frequency duplex division
V2V	vehicle to vehicle
TDD	time duplex division
DL	downlink
UL	uplink
RF	radio frequency
LTE-PRO	long term evolution - professional

CSI-RS	channel state information reference signals
SINR	signal to interference noise ratio
DFT	discrete Fourier transform
RL	reverse link
FL	forward link
SCEIA	spatial channel estimation for interference alignment
AoA	angle of arrival
AoD	angle of departure
LoS	line of sight
NLoS	non line of sight
MMSE	minimum mean squared error
MSE	mean square error
BER	bit error rate
3GPP	3rd generation partnership project
SR	sum rate
QP-IA	quantized precoder interference alignment
SM	spatial modulation
FMMSCE	FDD massive MIMO spatial channel estimation
SVD	singular value decomposition
EVD	eigen value decomposition
FFT	fast Fourier transform
SNR	signal to noise ratio
ORG	overhead reduction gain
CCE	channel covariance estimation

H-CSI	hybrid channel state information
P-CSI	progressive channel state information
SBEM	spatial basis expansion model
UMA	urban macro
TM3	transmission mode 3
CVQ	conventional vector quantization
CQG	channel quantization gain
FD	full dimensional
KP	Kronecker product
D-SCE	directional spatial channel estimation
URA	uniform linear array
EoD	elevation of departure
EoA	elevation of arrival
ECDF	empirical cumulative density function
E-CSI-RS	enhanced channel state information reference signals
RVQ	random vector quantization

Co-authorship Statement

I, Ali AbdulMawgood Ali Ali Esswie, have the principal author status for all the manuscripts included in this thesis. However, all manuscripts in this work are co-authored by my supervisors Dr. Octavia A. Dobre and Dr. Salama Ikki, in addition to other co-researchers, who have valuable contributions which facilitated the development of this work. The list of the manuscripts included in this thesis are described as below.

1. A. A. Esswie, M. El-Absi, O. A. Dobre, S. Ikki and T. Kaiser, "Spatial channel estimation-based FDD-MIMO interference alignment systems," *IEEE Commun. Lett.*, vol. 6, no. 2, pp. 254-257, April 2017

2. Ali A. Esswie, Mohammed El-Absi, Octavia A. Dobre, Salama Ikki and Thomas Kaiser, "A novel FDD massive MIMO system based on downlink spatial channel estimation without CSIT," in *Proc. IEEE ICC*, Paris, 2017, pp. 1-6.

3. Ali A. Esswie, Octavia A. Dobre, and S. Ikkir, "Directional Spatial Channel Estimation For Massive FD-MIMO in Next Generation 5G Networks," *Submitted to IEEE Signal Process. Lett.*, July 2017.

Ali AbdelMawgood Ali Ali Esswie

July 2017

Chapter 1

Introduction

1.1 Motivation

Wireless communications have gone through significant evolution over the past decade, to support ultra-high data rates, low-latency and seamless communications. The demand for wireless data services is growing by 2.0 times every year [1] due to the progressive increase of wireless mobile applications. With the ongoing advancement of future communication technology such as internet of everything (IoEs), vehicle to vehicle (V2V) communications, and big data, the next generation 5G cellular networks are expected to support significant traffic and user capacity [2], which current fourth generation (4G) technology can not provide. One of the major limitations of the cellular communications is the residual interference, e.g., inter-user, inter-cell, and inter-carrier interference. Thus, interference mitigation and cancellation have always been a key focus of the wireless standards [3-5].

However, despite the significant performance gains, these interference mitigation techniques [3-5] require full or partial channel state information at transmitter (CSIT), for the base-station (BS) to properly design a signal which adds constructively in the

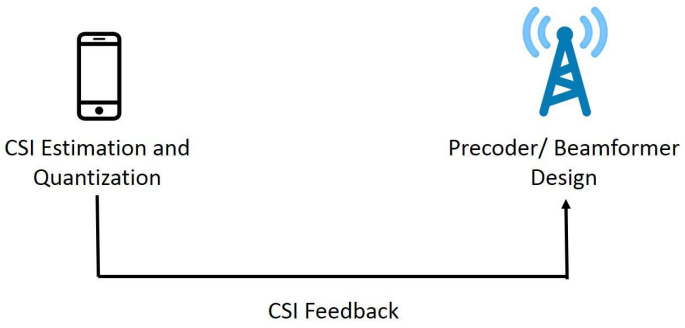

Figure 1.1: CSI estimation and quantization in FDD cellular communications.

direction of the intended users and destructively towards the interfering users, as depicted in Figure 1.1. In time division duplex (TDD) systems, the downlink (DL) and uplink (UL) links are modulated over the same frequency band. Hence, the channel can be considered reciprocal in both directions, where the DL channel is approximated by the transpose of the UL channel, providing the BS with an access to the DL channel information [6]. Though, in frequency division duplex (FDD) systems, the UL and DL channels are modulated over different carriers, to boost the overall capacity, which ultimately means that the DL and UL are not in fact reciprocal [6].

In FDD systems, the BS transmits periodic training pilots in the DL direction for facilitating the DL channel estimation at the user equipment's (UEs). Then, each UE estimates its corresponding DL channel, quantizes it through a pre-known codebook, and feeds-back its serving BS with an index to indicate the closest match codeword from the codebook [7-9]. Furthermore, due to the fact that the wireless channels are time-varying, this process is repeated every channel coherence time as depicted in Figure 1.2. Hence, the DL training pilots and UL feedback overhead are considered a fundamental limitation of cellular communications [10], e.g., attaining high precision CSIT leads to overwhelming feedback overhead, which significantly reduces the network spectral efficiency (SE). To effectively benefit from such advanced interference mitigation techniques, the CSIT acquisition overhead should be carefully

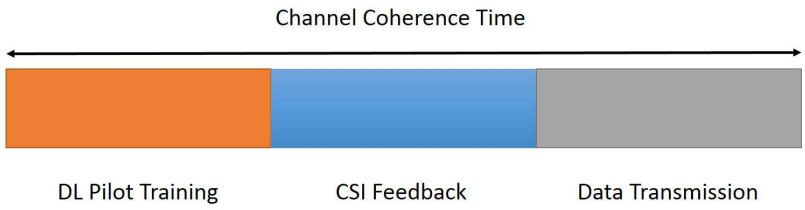

Figure 1.2: Periodic CSIT flow in FDD cellular communications.

taken into account in designing a cellular system.

In this thesis, we develop a novel CSIT acquisition strategy which blindly achieves near-perfect-CSIT performance with zero feedback overhead. We first consider the proposed strategy in the multi-input multi-output (MIMO) interference alignment (IA) systems, with practical channel modeling [7]. IA is known to achieve the maximum spatial degrees of freedom (DoFs) of the MIMO interference networks. Thus, it is considered a strong candidate for 5G cellular technology. However, IA is demonstrated to be sensitive to the quality of the CSIT. Hence, most of the IA studies consider high CSIT overhead load, e.g., 20/30 bits per user per channel coherence time, which is non-feasible in practice. Thus, we establish a strategy for CSIT acquisition in MIMO-IA systems which incorporates high performance CSIT, zero-bit feedback overhead, and *on-the-go* beamforming gain.

Furthermore, we consider the CSIT acquisition problem in massive MIMO (mMIMO) systems, where the BS is equipped with a large number of antennas, providing tremendous capacity gains [10]. However, in mMIMO systems, the size of the feedback overhead scales linearly with the number of transmit antennas, which is considered to be a fundamental limitation against implementing DL mMIMO communications in FDD networks. The majority of the current standardized solutions suffer from scalability issues with the number of the transmit antennas. Thus, the CSIT acquisition in DL mMIMO systems still remains an open question. With our proposed scheme, mMIMO systems are relieved from the bottleneck of the DL channel quantization and UL feed-

back overhead, with practical channel modeling. Finally, we extend our proposed scheme to the full dimensional space, where a more realistic 3D user distribution is considered and the attained CSIT is harvested in both the azimuthal and elevation directions [11].

1.2 Literature Review and Background

Harvesting accurate CSIT has always been a crucial challenge against all wireless communication channels [12]. A typical spatial wireless channel is known to be a multi-path channel, where the communication link between a BS and UE is composed from several channel paths with different gains and delays [13]. Thus, the BS requires knowledge of each user's CSI to precode its corresponding traffic into the principal paths of its DL channel. Ideally, and to achieve the optimal performance of the MIMO technology, CSIT of each UE should be perfectly known at BS [14]. However, the DL channel information is only available at the UE side. In literature, there are two major frameworks for harvesting CSIT, which depend on the communication system itself. In TDD systems, the UL and DL channels are modulated over the same frequency band; as a result, the channel principal clusters become highly correlated [15]. Thus, the typical precoding schemes in TDD systems reasonably assume channel reciprocity, where the DL channel can be approximated by the transpose of the UL channel, eliminating the need for additional CSIT harvesting overhead [16-18]. On the other hand, in FDD systems, the DL and UL channels are modulated over separated frequency bands. Hence, the principal channel directions may deviate from each other, which in turn, introduces the need for a limited feedback from every UE [19-21]. However, in practice, FDD systems are most widely implemented due to the higher provided data rates and the low complexity of the radio frequency (RF) transmission.

Thus, the current majority of the CSIT harvesting contributions are aimed towards FDD systems.

In FDD-MIMO systems, there is always a tradeoff between the size of the user feedback overhead, precision of the attainable CSIT, and the complexity of implementation [22]. In current standards of the LTE-Pro [23], a training based CSIT harvesting strategy is adopted due to the low implementation complexity at the BS and UE sides. However, it comes with the expense of additional CSI feedback overhead per channel coherence time. Double codebooks are predefined at both BS and UE. The first codebook tracks the slow varying channel characteristics, while the second codebook tracks the small-scale channel characteristics. The BS shoots several DL pilots over pre-designed time-frequency resources for the UE to estimate its DL channel. Then, each UE approximates its estimated DL channel by the closest codewords from the double codebooks, and finally it feeds-back its serving BS with two indices of the selected dual codewords. Different feedback periodicity are being defined to minimize the overall feedback overhead, e.g., 80 ms and 5 ms for the first and second codebooks, respectively. Thus, the training-based CSIT harvesting in FDD-MIMO systems has been widely investigated in literature [24, 25], due to the low implementation complexity. It was theoretically shown that the training-based CSIT is asymptotically optimal, when the size of the codebook tends to be very large [26], providing large spatial scanning precision of the antenna sector. This leads to overwhelming feedback overhead, which scales linearly with the number of antenna elements at the BS, and hence, consumes the UL channel capacity accordingly. Thus, training-based CSIT harvesting schemes are not usually recommended for massive MIMO systems or with 3D beamforming, where massive feedback overhead may be needed.

For 3D massive MIMO systems, CSIT harvesting problem is additionally chal-

lenged by the scalability issues with the large antenna arrays and the feedback dimensionality (elevation/ azimuthal). The current standardized double codebooks have been extended to scan the horizontal in addition to the vertical cell coverage space, providing a Kronecker-product based beamforming scheme for 3D channels [27, 28]. Though, it has been shown that Kronecker-product (KP) based beamforming is not scalable with the number of transmit antennas, e.g., adopting very large antenna arrays with moderate codebook sizes, and hence moderate feedback overhead, does not lead to a remarkable performance enhancement, due to the limited quantization spatial DoFs. Another promising framework for attaining 3D CSIT is the beamformed CSI reference signals (CSI-RS), where the DL pilots are beamformed towards predefined directions, to cover the 3D space of each cell [29, 30]. Each UE feeds-back its serving BS with an index of its principal pilot direction for data beamforming. Due to the beamforming and array gains, the beamformed CSI-RS tends to provide a better performance than the KP-based beamforming, e.g., extended coverage with higher levels of the signal-to-interference-noise-ratio (SINR). Additionally, the CSI-RS pilots are generated by the discrete Fourier transform (DFT), and thus, the engineering practical limitations such as the constant modulus and the fixed alphabet size, can be satisfied. However, with lower scanning precision, CSI-RS schemes may result in blind coverage spots, where users are sub-optimally served by beam-side-lobes. A diversity of extensions of the CSI-RS CSIT has been proposed to tradeoff performance with complexity, such as the rotated CSI-RS [31, 32].

On another side, the most practical MIMO transceivers fall under two major categories as follows:

1. **Linear transceivers**: Each transmitted data stream is estimated through a linear combination of the received signals across the antenna elements. This category includes the zero-forcing (ZF), and the minimum mean square error

(MMSE) transceivers.

2. **Non-linear transceivers**: Each transmitted data stream is estimated through an iterative successive interference cancellation (SIC) algorithm.

The spatial matched filter (SMF) is a basic MIMO transceiver. SMF depends on processing the received signal by focusing as much energy as possible towards the direction of the desired stream; however, without control on the inter-stream interference levels. The received signal at the output of the SMF for the $\mathcal{L}^{th}$ stream is given by

$$y_{\mathcal{L}} = \| \mathrm{h}_{\mathcal{L}} \|^2 \, s_{\mathcal{L}} + \sum_{i \neq \mathcal{L}} \mathrm{h}_{\mathcal{L}}^{\mathrm{Herm.}} \mathrm{h}_i s_i + \mathrm{h}_{\mathcal{L}} \boldsymbol{n}, \tag{1.1}$$

where Herm. indicates the Hermitian matrix operation, $\mathbf{F}_{smf} = \mathrm{h}_{\mathcal{L}}$ denotes the SMF transfer function, $s_{\mathcal{L}}$ is the desired data stream, and $\boldsymbol{n}$ is the Gaussian noise. The summation term indicates the inter-stream interference. The SMF provides the least filtering complexity; however, it provides poor performance when the inter-stream interference is significant.

However, the ZF transceiver completely eliminates the inter-stream interference by inverting the MIMO channel matrix as,

$$\mathbf{F}_{zf} = \frac{1}{\mathbf{H}}, \tag{1.2}$$

where $\mathbf{H}$ is the MIMO channel matrix. Ideally, the low-magnitude channel samples are compensated by larger filter response and the large magnitude channel samples are compensated by lower filter response to provide a unity response of the transmitted data streams. However, due to the inversion operation, ZF suffers from the noise enhancement problem, in the low signal strength region.

The MMSE transceiver aims to minimize the average estimation error of each

data stream. Unlike the ZF, the average error is considered over both the transmitted data and the corresponding noise, to overcome the noise enhancement problem. The transfer function of the MMSE transceiver is given by

$$\mathbf{F}_{mmse} = \left(\mathbf{H}^{\text{Herm.}} \mathbf{H} + \frac{\sigma_n^2}{P} \boldsymbol{I} \right) \mathbf{H}^{\text{Herm.}}, \tag{1.3}$$

where σ_n^2 is the noise variance. On the other side, the SIC transceiver provides the best achievable performance with the expense of the processing complexity. SIC is an iterative transceiver, where the number of the interfering streams is reduced by one every iteration. Table 1.1 summarizes the achievable capacity of the MIMO channel with the SMF, ZF, MMSE, and SIC transceivers. Figure 1.1 shows the spectral efficiency comparison of the listed transceivers, for the 32×2 antenna setup. It shows that the ZF approaches the MMSE in the high signal-to-noise (SNR) ratio, where poor noise levels exist. Additionally, the MF shows the worst performance since the inter-stream interference is mistreated as noise. Generally, linear transceivers are the most widely used in MIMO systems, because of the low processing complexity. However, they suffer from sub-optimal performance, due to the limited DoFs in high interference environments. Thus, linear transceivers are known to provide lower multi-user capacity than non-linear transceivers.

Interestingly, the capacity variance of the MIMO channel shrinks with the number of BS antennas, e.g., the diagonal channel coefficients approach unity, while the off diagonal coefficients approach zero. This phenomenon is known as "channel hardening", where the desired channel coefficients become more predominant with the number of the BS antennas, as shown in Figure 1.2 for different antenna setups. Channel hardening is considered as self-interference-mitigation in massive MIMO systems, where linear transceivers become sufficient to achieve near optimal performance, with the near-orthogonal channels.

Table 1.1: MIMO channel capacity with SMF, ZF, MMSE, and SIC transceivers.

Transceiver	SINR (i^{th} user)
Spatial matched filter (SMF)	$\frac{p_i \|h_i\|^2}{\sum_{j \neq i} \|\mathrm{h}_j^{\mathrm{Herm.}} h_i\|^2 + \sigma^2}$
Zero-forcing (ZF)	$\frac{p_i}{\sigma^2 \left(\mathbf{H}^{\mathrm{Herm.}} \mathbf{H}\right)^{-1}}$
Minimum mean square error (MMSE)	$\frac{p_i}{\sigma^2 \left(\mathbf{H}^{\mathrm{Herm.}} \mathbf{H} + \frac{\sigma^2}{p_i}\right)^{-1}} - 1$
Successive interference cancellation (SIC)	$\frac{p_i}{\sigma^2} \left(\mathbf{H}^{\mathrm{Herm.}} \mathbf{H}\right)$

Thus, with large antenna arrays, high spatial correlation between the DL and UL channels is observed, based on many channel field measurements campaigns [33-35], due to the small difference between the angular spread of both channels. Blind CSIT harvesting schemes are proposed to utilize the spatial correlation of the UL and DL channels, and to obtain an accurate CSIT, without the need for extensive feedback overhead. Llyod [36], local-packing [37], Grassmannian-subspace-packing [38], and individual-gain-and-phase-quantification [39] algorithms are known to generate time-updated codebooks for 3D channels. However, the knowledge of the local and/or global user channel covariance matrices are required for the blind processing. Thus, the large antenna array dimension leads to high processing complexity in the matrix operations.

A blind and scalable CSIT scheme, which provides an accurate CSIT harvesting gain, and complies with the practical limitations such as the constant modulus, fixed alphabet, and the lower computational complexity, is still vital for 3D massive FDD-MIMO systems.

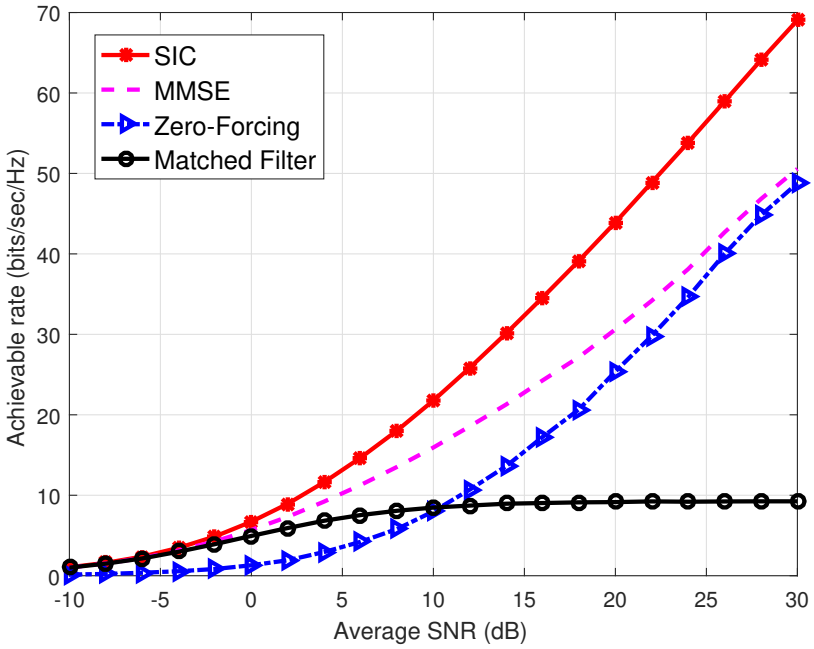

Figure 1.1: MIMO spectral efficiency with SMF, ZF, MMSE, and SIC transceivers.

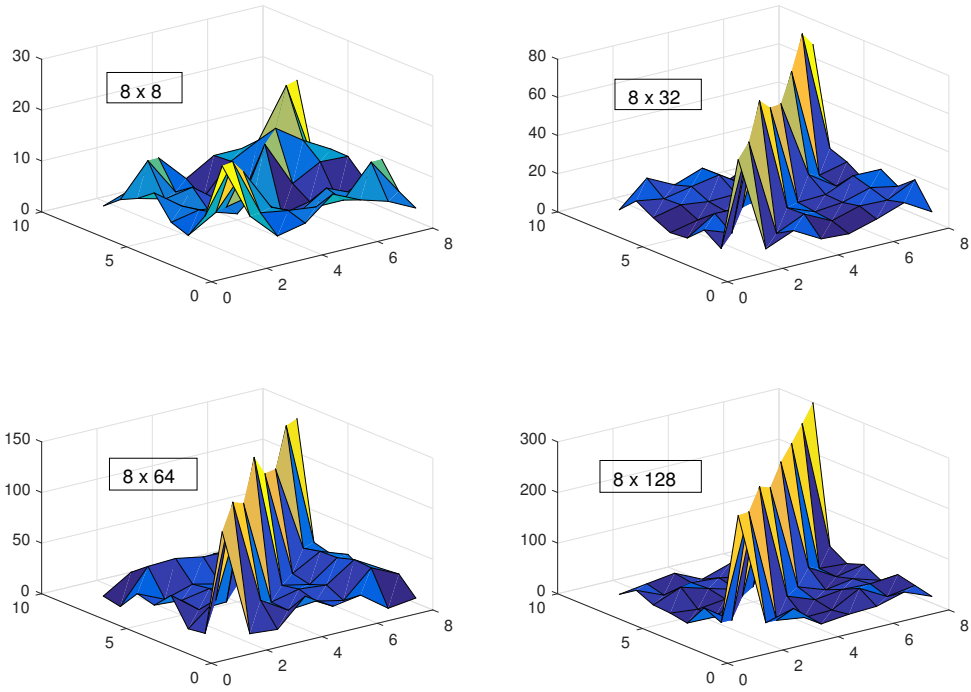

Figure 1.2: Channel hardening phenomenon in massive MIMO networks.

1.3 Thesis Outline and Contribution

Based on the previous discussion, the following observations can be noted:

1. Most of the CSIT investigations in recent literature consider independent and identically distributed (i.i.d.) Rayleigh fading channels, which facilitates achieving closed form rate expressions. However, practical channels are not spatially uncorrelated, based on diversity of field measurement campaigns, in which these rate expressions are unachievable in practical deployments.

2. Interference is a fundamental limitation in cellular communications. Advanced interference mitigation techniques require large loads of user feedback overhead and channel quantization, e.g., 20/ 30 control bits per user per channel coherence time. Thus, this requirement significantly degrades the overall system performance, where large segments of the network resources are consumed by control feedback.

3. Massive MIMO (mMIMO) communication, where a large antenna array is adopted at transmitter, is a key technology for the upcoming 5G cellular communications. mMIMO has been demonstrated to allow for simple and linear interference mitigation transceivers, while achieving near optimal performance. However, the amount of user feedback overhead must be scaled linearly with the number of transmit antennas, which is considered a critical limitation against the practical implementation of the mMIMO systems. Recent mMIMO studies are either to consider high user feedback control overhead or to perform high-complexity blind CSIT acquisition, incorporating several unreasonable assumptions in practice.

4. Full dimensional mMIMO communications are more realistic in practical deployments, where connected capacity is distributed in both the azimuthal and

elevation directions. Thus, the CSIT acquisition problem becomes more challenging, where the optimal performance is achieved only by full load of the user feedback overhead in both directions. This leads to significant loss in the system spectral efficiency, yielding the full dimensional massive MIMO systems not yet to be incorporated in current standards.

Motivated by the aforementioned observations, we addressed the following issues:

1. Developing a blind CSIT acquisition strategy for advanced interference alignment schemes, without channel quantization, and user feedback overhead over multi-user MIMO channels. The standardized and practical spatial channel modeling is incorporated instead of the theoretical i.i.d. channels.

2. Developing a novel CSIT acquisition scheme which is scalable to mMIMO systems, without the limitations of the DL channel quantization and the non-stationary channel characteristics, which are presented when using large antenna arrays.

3. Attaining high-precision CSIT in full dimensional systems, without quantization limitation in either the azimuthal or elevation directions.

In Chapter 2, we introduce a spatial channel estimation algorithm for MIMO-IA systems. Unlike the current IA investigations, we approached the SE of the perfect-CSIT, where the exact channels are known at the BS, without the requirements of channel quantization or feedback overhead.

In Chapter 3, we extend our system model to an FDD massive MIMO system, to utilize the great offered spatial DoFs in the blind estimation algorithm. Results show that the proposed CSIT strategy is effective with large antenna arrays, compared to recent algorithms from industry and academia.

In Chapter 4, we consider the full-dimensional channel modeling, where more practical deployment scenarios are considered. The simulation results show that our algorithm outperforms the state-of-the-art schemes in current wireless standards.

Finally, thesis conclusion and potential future developments are presented in **Chapter 5**.

References

[1] "Global Mobile Data Traffic Forecast Update, 2015 – 2020", CISCO, 2017.

[2] M. Ptzold, "5G developments are in full swing [Mobile Radio]," *IEEE Veh. Technol. Mag.*, vol. 12, no. 2, pp. 4-12, June 2017.

[3] C. Yang, J. Li, Q. Ni, A. Anpalagan and M. Guizani, "Interference-aware energy efficiency maximization in 5G ultra-dense networks," *IEEE Trans. Commun.*, vol. 65, no. 2, pp. 728-739, Feb. 2017.

[4] S. Hamid, A. J. Al-Dweik, M. Mirahmadi, K. Mubarak and A. Shami, "Inside-out propagation: developing a unified model for the interference in 5G networks," *IEEE Veh. Technol. Mag.*, vol. 10, no. 2, pp. 47-54, June 2015.

[5] T. Y. Wu and T. Chang, "interference reduction by millimeter wave technology for 5G-based green communications," *IEEE Access*, vol. 4, pp. 10228-10234, 2016.

[6] X. Jiang, M. Čirkić, F. Kaltenberger, E. G. Larsson, L. Deneire and R. Knopp, "MIMO-TDD reciprocity under hardware imbalances: Experimental results," *in Proc. IEEE ICC*, London, 2015, pp. 4949-4953.

[7] A. A. Esswie, M. El-Absi, O. A. Dobre, S. Ikki and T. Kaiser, "Spatial channel estimation-based FDD-MIMO interference alignment systems," *IEEE Commun. Lett.*, vol. 6, no. 2, pp. 254-257, April 2017.

[8] Y. Han, W. Shin and J. Lee, "Projection-based differential feedback for FDD massive MIMO systems," *IEEE Trans. Veh. Technol.*, vol. 66, no. 1, pp. 202-212, Jan. 2017.

[9] J. Song, J. Choi, K. Lee, T. Kim, J. y. Seol and D. J. Love, "Advanced quantizer designs for FD-MIMO systems using uniform planar arrays," *in Proc. IEEE GLOBECOM*, Washington, DC, 2016, pp. 1-6.

[10] Ali A. Esswie, Mohammed El-Absi, Octavia A. Dobre, Salama Ikki and Thomas Kaiser, "A novel FDD massive MIMO system based on downlink spatial channel estimation without CSIT," in *Proc. IEEE ICC*, Paris, 2017, pp. 1-6.

[11] Ali A. Esswie, Octavia A. Dobre, and Salama Ikki, "Directional spatial channel estimation for massive FD-MIMO in next generation 5G networks," *to be submitted.*

[12] T. L. Marzetta, G. Caire, M. Debbah, I. Chih-Lin, and S. K. Mohammed, "Special issue on massive MIMO," *J. Commun. Netw.*, vol. 15, no. 4, pp. 333–337, 2013.

[13] Study on 3D channel model for LTE," 3GPP, TR 36.873, Sep. 2014.

[14] L. Berriche, K. Abed-Meraim, and J.-C. Belfiore, "Investigation of the channel estimation error on MIMO system performance," *in Proc. EUSIPCO*, Antalya, Turkey, Sep. 2005, pp. 1–4.

[15] T. Marzetta, "How much training is required for multi user MIMO?" *in Proc. ACSSC*, Oct. 2006, pp. 359–363.

[16] J. Hoydis et al., "Massive MIMO in the UL/DL of cellular networks: How many antennas do we need?" *IEEE J. Sel. Areas Commun.*, vol. 31, no. 2, pp. 160–171, Feb. 2013

[17] J. Jose, A. Ashikhmin, T. Marzetta, and S. Vishwanath, "Pilot contamination and precoding in multi-cell TDD systems," *IEEE Trans. Wireless Commun.*, vol. 10, no. 8, pp. 2640–2651, Aug. 2011

[18] T. Marzetta and B. Hochwald, "Fast transfer of channel state information in wireless systems," *IEEE Trans. Signal Process.*, vol. 54, no. 4, pp. 1268–1278, Apr. 2006

[19] Y. Yu and D. Gu, "Enhanced MU-MIMO downlink transmission in the FDD-based distributed antennas system," *IEEE Commun. Lett.*, vol. 16, no. 1, pp. 37–39, Jan. 2012.

[20] J. Chang, I. Lu, and Y. Li, "Adaptive codebook-based channel prediction and interpolation for multiuser multiple-input multiple-output orthogonal frequency division multiplexing systems," *IET Commun.*, vol. 6, no. 3, pp. 281–288, Feb. 2012.

[21] A. Rajanna and N. Jindal, "Multiuser diversity in downlink channels: When does the feedback cost outweigh the spectral efficiency benefit?" *IEEE Trans. Wireless Commun.*, vol. 11, no. 1, pp. 408–418, Jan. 2012.

[22] G. Taricco and E. Biglieri, "Space-time decoding with imperfect channel estimation," *IEEE Trans. Wireless Commun.*, vol. 4, no. 4, pp. 1874– 1888, Jul. 2005

[23] T. Shuang, T. Koivisto, H. L. Maattanen, K. Pietikainen, T. Roman and M. Enescu, "Design and Evaluation of LTE-Advanced Double Codebook," *in Proc. VTC*, Yokohama, 2011, pp. 1-5.

[24] L. Tong, B. M. Sadler, and M. Dong, "Pilot-assisted wireless transmissions: general model, design criteria, and signal processing," *IEEE Signal Process. Mag.*, vol. 21, no. 6, pp. 12–25, Nov. 2004

[25] M. Coldrey and P. Bohlin, "Training based MIMO systems—Part I : Performance comparison," *IEEE Trans. Signal Process.*, vol. 55, no. 11, pp. 5464–5476, Nov. 2007.

[26] M. Coldrey and P. Bohlin, "Training Based MIMO systems—Part II: improvements using detected symbol information," *IEEE Trans. Signal Process.*, vol. 56, no. 1, pp. 296–303, Jan. 2008.

[27] Y. Xie, S. Jin, J. Wang, Y. Zhu, X. Gao, and Y. Huang, "A limited feedback scheme for 3D multiuser MIMO based on kronecker product codebook," *in Proc. IEEE PIRMC*, London, 2013, pp. 1130-1135..

[28] D. Yang, L.-L. Yang, and L. Hanzo, "DFT-based beamforming weight-vector codebook design for spatially correlated channels in the unitary precoding aided multiuser downlink," *in Proc. IEEE Int. Communi. Conf.*, 2010

[29] Y. Song, S. Nagata, H. Jiang and L. Chen, "CSI-RS design for 3D MIMO in future LTE-advanced," *in Proc. ICC*, Sydney, NSW, 2014, pp. 5101-5106.

[30] Precoding Schemes for Elevation Beamforming and FD-MIMO, NTT DOCOMO, 3GPP, TSG RAN WG1, MEETING # 80: R1-151983, 2015.

[31] A. Esswie and A. Fouda, "Three-dimensional progressive rotated codebook for advanced multi-user MIMO in LTE-A networks," *in Proc. ATC*, Ho Chi Minh City, 2015, pp. 20-25.

[32] M. Sajadieh, A. Esswie, A. Fouda, H. Shirani-Mehr and D. Chatterjee, "Progressive channel state information for advanced multi-user MIMO in next generation cellular systems," *in Proc. WCNC*, Doha, 2016, pp. 1-6.

[33] M. Narandzic, C. Schneider, R. Thoma, T. Jamsa, P. Kyosti and X. Zhao, "Comparison of SCM, SCME, and WINNER Channel Models,"*in Proc. VTC-Spring*, Dublin, 2007, pp. 413-417.

[34] B. Clerckx, G. Kim, and S. Kim, "Correlated fading in broadcast MIMO channels: Curse or blessing?" *in Proc. IEEE GLOBECOM*, New Orleans, LO, 2008, pp. 1-5.

[35] A. Adhikary, J. Nam, J.-Y. Ahn, and G. Caire, "Joint spatial division and multiplexing the large-scale array regime," *IEEE Trans. Inform. Theory,* vol. 59, no. 10, pp. 6441–6463, Oct. 2013.

[36] H. Abut, Vector quantization, 1st ed. New York: IEEE Press, 1990.

[37] V. Raghavan, R. W. Heath Jr., and A. M. Sayeed, "Systematic codebook designs for quantized beamforming in correlated MIMO channels," *IEEE J. Select. Areas Commun.*, vol. 25, no. 7, pp. 1298–1310, Sep. 2007.

[38] Y. Huang, L. Yang, M. Bengtsson, and B. Ottersten, "Exploiting long-term channel correlation in limited feedback SDMA through channel phase codebook," *IEEE Trans. Signal Process.*, vol. 59, no. 3, pp. 1217–1228, Mar. 2011.

[39] J. Choi, V. Raghavan, and D. J. Love, "Limited feedback design for the spatially correlated multi-antenna broadcast channel," *in Proc. IEEE GLOBECOM*„ Atlanta, GA, 2013, pp. 3481-3486.

Chapter 2

Spatial Channel Estimation for FDD MIMO-IA Systems*

2.1 Abstract

The practical feasibility of interference alignment (IA) is a major challenge in real-world implementation. The majority of the research contributions assume ideal channel reciprocity, which may be valid in time division duplex (TDD) systems. In frequency division duplex (FDD) systems, large codebooks are utilized for channel quantization, which consume the feedback channel capacity. In this work, a spatial channel estimation method is proposed for FDD-MIMO IA systems. The method utilizes the path correlation between the forward and reverse channels, where channels are on different frequency bands. A transformation matrix is employed to estimate the angles of departure of the forward channel. The proposed method shows a significant improvement of the sum rate without the need of feedback overhead bits.

*This chapter is a modified version of "A. A. Esswie, M. El-Absi, O. A. Dobre, S. Ikki and T. Kaiser, "Spatial channel estimation-based FDD-MIMO interference alignment systems," *IEEE Commun. Lett.*, vol. 6, no. 2, pp. 254-257, April 2017"

Index Terms— Interference alignment; Reciprocity; MIMO; Channel state information; Feedback.

2.2 Introduction

INTERFERENCE alignment (IA) can achieve the maximum multiplexing gain over MIMO channels. IA designs the signals at transmitters to be aligned in a signal subspace at receivers, leaving the other interference-free subspace for desired signal transmission [1, 2, 3]. IA has proven that interference is not a fundamental limitation in a K-user MIMO interference channel. In [3], the sum capacity of the K-user interference channel under IA is shown to scale linearly with the number of connected users.

The IA closed-form solution requires global channel state information at the transmitters (CSIT) in order to cooperatively design the precoder and decoder vectors [4], which is not feasible in practice. Feasible solutions such as iterative algorithms are proposed in the literature that require only local CSIT [5]. A widely used IA algorithm is the maximum signal-to-interference noise ratio (SINR). It provides the optimal IA degrees of freedom (DoFs) with well scaled-complexity. However, the maximum SINR criterion is shown to be sensitive to the accuracy of the estimated channels [6, 7].

Therefore, the majority of contributions assume ideal reciprocity, where the channels of the reverse link (RL) and forward link (FL) are assumed to be reciprocal. However, channel reciprocity is not valid in FDD systems. Thus, CSI quantization algorithms are proposed to enhance the attainable CSIT precision under B-bit limited-feedback per channel coherence time [8, 9]. Nevertheless, a slight mismatch between the actual and quantized FL channels leads to significant performance degradation. With inaccurate channel estimation at the transmitter, the maximum SINR criterion

improperly designs the transmission precoders, which results in non-aligned interference at receivers. To enhance the CSIT accuracy, current solutions employ large codebooks, with a large number of feedback overhead bits, e.g., 20 bits [10].

In this chapter, a spatial channel estimation method for MIMO IA systems (SCEIA) is proposed for FDD communications. SCEIA projects the RL channel, known from the RL sounding [12], on a set of predefined channel directions, which forms a codebook that spans the entire coverage of the antenna sector. The channel directions in the codebook are compensated by the frequency gap between the RL and FL channels. The spatial power spectrum is obtained and a vector of the principal FL angles of departure (AoDs) is estimated, based on the RL angles of arrival (AoAs). The FL channel is estimated through a transformation matrix in terms of the estimated AoDs. Thus, the overall performance is not fundamentally limited by the FL channel quantization accuracy, and the proposed method requires no feedback overhead bits, e.g., $B = 0$ bits.

This chapter is organized as follows. Section 2.3 describes the system model. Section 2.4 introduces the proposed SCEIA method. Simulation results are presented in Section 2.5 and conclusions are drawn in Section 2.6.

2.3 System Model

In this work, we consider a MIMO ad-hoc interference network with K transmitter-receiver pairs. All transmitters and receivers are equipped with N_t transmit antennas and M_r receive antennas, respectively, as shown in Figure 2.1. The i^{th} receiver desires to accommodate d_i independent data streams $s_i = \boldsymbol{\mathcal{CN}}(0, \frac{P}{d_i}\mathbf{I}_{d_i})$. The channel matrix from the j^{th} transmitter to the i^{th} receiver is denoted by $\mathbf{H}_{ij} \in C^{M_r \times N_t}, \forall i, j \in \{1, 2, \ldots, K\}$.

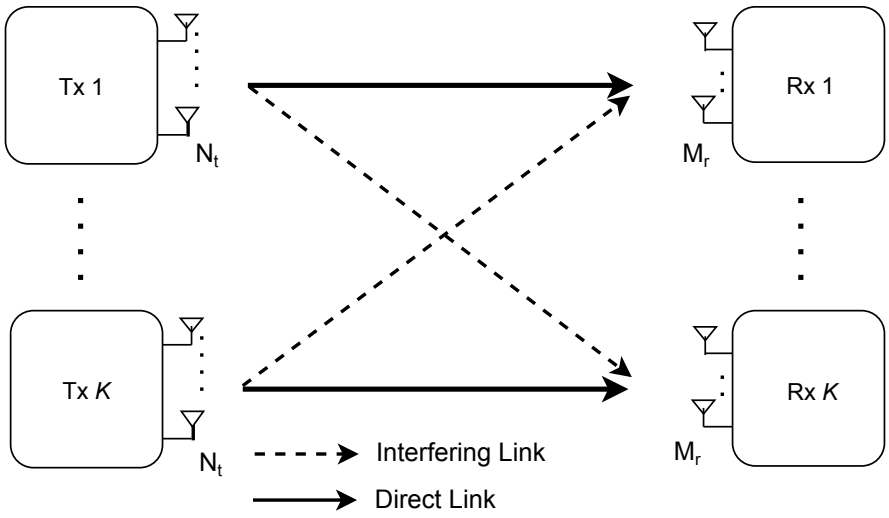

Figure 2.1: K transmitter-receiver pairs over ad-hoc MIMO interference channel.

The precoder vectors at transmitters and decoder vectors at receivers are designed and updated to satisfy the IA objective function and are denoted by $\mathbf{V}_j = [\mathbf{v}_j^1 \mathbf{v}_j^2 \dots \mathbf{v}_j^{d_i}] \in C^{N_t \times d_i}$ and $\mathbf{U}_i = [\mathbf{u}_i^1 \mathbf{u}_i^2 \dots \mathbf{u}_i^{d_i}] \in C^{M_r \times d_i}$ respectively, where $\mathbf{v}_j^p$ and $\mathbf{u}_i^p, \forall p \in \{1, 2, \dots, d_i\}$ are the corresponding column vectors of the precoders and decoders with respect to each single data stream between the $j^{th} - i^{th}$ transmitter-receiver pair. Hence, the discrete-time received p^{th} stream at the i^{th} user is given by

$$\boldsymbol{y}_i^p = \mathbf{H}_{ii}\mathbf{v}_i^p\mathbf{s}_i^p + \sum_{l=1, l\neq p}^{d_i} \mathbf{H}_{ii}\mathbf{v}_i^l\mathbf{s}_i^l + \sum_{j=1, j\neq i}^{K} \sum_{m=1}^{d_j} \mathbf{H}_{ij}\mathbf{v}_j^m\mathbf{s}_j^m + \mathbf{n}_i, \tag{2.1}$$

where $\boldsymbol{n}_i$ is the additive white Gaussian noise at the i^{th} user. The first and second summation terms represent the intra-user inter-stream and the inter-user interference, respectively. To reconstruct the p^{th} stream at the i^{th} user, the p^{th} stream received signal is decoded using an orthonormal receive suppression filter $\mathbf{u}_i^p$. The reconstructed data stream $\hat{\mathbf{s}}_i^p$ at the i^{th} receiver can be written as

$$\hat{\mathbf{s}}_i^p = (\mathbf{u}_i^p)^{\mathrm{H}} \boldsymbol{y}_i^p, \tag{2.2}$$

where the superscript H denotes the Hermitian transpose operation. For perfect interference alignment at the i^{th} receiver, the following conditions must be satisfied:

$$\mathbf{U}_i^{\mathrm{H}}\mathbf{H}_{ij}\mathbf{V}_j = 0, \forall i \neq j \tag{2.3}$$

$$\mathrm{rank}\{\mathbf{U}_i^{\mathrm{H}}\mathbf{H}_{ii}\mathbf{V}_i\} = d_i, \tag{2.4}$$

and the achievable sum rate at the i^{th} receiver is expressed as

$$R_i = \log_2 \left| \mathbf{I} + \frac{\mathbf{U}_i^{\mathrm{H}}\mathbf{H}_{ii}\mathbf{V}_i\mathbf{H}_{ii}^{\mathrm{H}}\mathbf{V}_i^{\mathrm{H}}\mathbf{U}_i}{\sum_{j=1,j\neq i}^{K}\mathbf{U}_i^{\mathrm{H}}\mathbf{H}_{ij}\mathbf{V}_j\mathbf{H}_{ij}^{\mathrm{H}}\mathbf{V}_j^{\mathrm{H}}\mathbf{U}_i + \sigma^2\mathbf{I}} \right|. \tag{2.5}$$

The 3GPP spatial channel model (SCM) is used in this work [11]. It is described by the strongest $C = 6$ clusters or reflections, each with 20 sub-paths for non-line of sight communications (NLoS). The SCM channel steering element from the s^{th} to u^{th} antenna on the q^{th} channel cluster is described by

$$h_{\{u,s,q\}} = \sqrt{\frac{p_q\sigma_{sf}}{20}} \sum_{z=1}^{20} \Big(\sqrt{G_T(\theta_{q,z,\mathrm{AoD}})} e^{j[k\nabla \sin(\theta_{q,z,\mathrm{AoD}})]}$$

$$\times \sqrt{G_R(\theta_{q,z,\mathrm{AoA}})} e^{j[k\nabla \sin(\theta_{q,z,\mathrm{AoA}})]} e^{jk||v||cos(\theta_{q,z,\mathrm{AoA}}-\theta_v)t} \Big) , \tag{2.6}$$

where p_q and σ_{sf} are the power and shadow fading factor of the qth sub-path, G_T and G_R are the transmitter and receiver antenna gains respectively, k is the wave number where $k = \frac{2\pi}{\lambda}$ and λ is the carrier wavelength, $\theta_{q,z,\mathrm{AoD}}$ and $\theta_{q,z,\mathrm{AoA}}$ are the FL AoD and RL AoA respectively, ∇ is the distance in meters between the s^{th} antenna and the reference antenna index, and v is the relative velocity. The channel matrix $\mathbf{H}_{ij}$ is expressed as

$$\mathbf{H}_{ij} = \frac{1}{\sqrt{C}} \begin{bmatrix} \sum_{q=1}^{C} h_{\{1,1,q\}} & \cdots & \sum_{q=1}^{C} h_{\{1,N_t,q\}} \\ \vdots & \ddots & \vdots \\ \sum_{q=1}^{C} h_{\{M_r,1,q\}} & \vdots & \sum_{q=1}^{C} h_{\{M_r,N_t,q\}} \end{bmatrix}. \tag{2.7}$$

2.4 Spatial Channel Estimation for IA Systems

In this section, the basic idea of the proposed SCEIA method is introduced. A set of predefined beamforming channel directions is generated with an arbitrary angle precision. These directions are compensated by the frequency gap between the RL and FL channels. The RL channel per user is energy-projected and the principal FL AoDs are captured. The FL channel is estimated through a two-step operation. A transformation matrix is constructed to provide a rough estimate by precoding the RL channel on the estimated FL AoDs. Then, the minimum mean square estimate (MMSE) of the FL channel is derived to refine the estimation accuracy.

2.4.1 Spatial Channel Estimation for FDD MIMO-IA Systems

The precoding and decoding vectors are updated at every pilot transmission to satisfy the maximization of the received SINR at the i^{th} receiver [1], which is given by

$$\mathrm{SINR}_i = \left(\frac{P}{d_i}\right) \frac{\mathbf{U}_i^{\mathrm{H}} \mathbf{H}_{ii} \mathbf{V}_i \mathbf{V}_i^{\mathrm{H}} \mathbf{H}_{ii}^{\mathrm{H}} \mathbf{U}_i}{\mathbf{U}_i^{\mathrm{H}} \mathbf{B}_{ij} \mathbf{U}_i}, i \neq j, \forall i, j \in \{1, \ldots, K\} \tag{2.8}$$

and the interference covariance matrix $\mathbf{B}_{ij}$ is expressed by

$$\mathbf{B}_{ij=} \sum_{j=1, j\neq i}^{K} \frac{P}{d_j} \sum_{l=1}^{d_j} \mathbf{H}_{ij} \mathbf{V}_j \mathbf{V}_j^{\mathrm{H}} \mathbf{H}_{ij}^{\mathrm{H}} + \mathbf{I}_i. \tag{2.9}$$

Ideally, the FL and RL channel clusters bounce on similar angle directions under

moderate mobility conditions, which depend on the frequency characteristics of both channels [11]. Therefore, widening the frequency gap between the RL and FL channels reduces the path correlation between the principal RL and FL channel clusters. As a result, the channel RL AoAs and FL AoDs start to deviate from each other.

Assuming an antenna sector of θ^o degrees of coverage, a set of N channel directions are generated to form a predefined codebook at the transmitter, where $N = \frac{\theta^o}{\rho}$ and ρ is an integer scaling factor. The codebook design is arbitrary for a given channel quantization precision. Without loss of generality, we consider $\theta^o = 120^o$, $\rho = 1$ and $N = 120$. Therefore, the codebook $\mathbf{F}(\theta_c), \forall c = 1, 2, \ldots, N$, is expressed as

$$\mathbf{F}(\theta_c) = \frac{1}{\sqrt{N_t}} \left[1, e^{-j2\pi \triangle_{\mathrm{RL}} \cos\theta_c}, \ldots, e^{-j2\pi \triangle_{\mathrm{RL}} (N_t - 1) \cos\theta_c}\right]^{\mathrm{T}}, \tag{2.10}$$

where the superscript T denotes the transpose operation, $\mathbf{F}(\theta_c)$ corresponds to the c^{th} beamformed channel direction from the codebook, which points to the direction of θ_c and $\triangle_{\mathrm{RL}}$ is the effective antenna spacing after compensating the frequency gap between RL and FL channels by the factor α,

$$\triangle_{\mathrm{RL}} = \alpha \triangle_{\mathrm{FL}}, \ \alpha = \frac{f_{\mathrm{RL}}}{f_{\mathrm{FL}}}, \tag{2.11}$$

where $\triangle_{\mathrm{FL}}$ is the FL antenna spacing in terms of the FL channel frequency, and f_{RL} and f_{FL} are the RL and FL channel carrier frequencies, respectively. The compensation factor α translates the frequency gap between the FL and RL channels into an effective antenna spacing to compensate for the difference in the channel path correlation. With a 4×4 antenna configuration, Figure 2.2 shows that the first estimated FL AoD approaches the actual channel AoD with average deviation of 2 degrees at SINR=10 dB. The estimation accuracy is shown to enhance with the SINR, as most of the signal energy is confined in fewer number of principal channel paths in the high

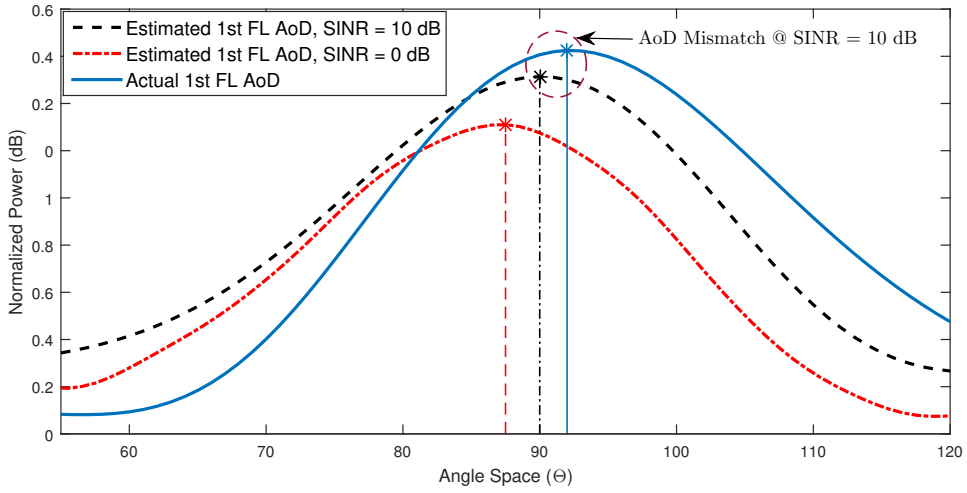

Figure 2.2: Estimation of the first principal FL AoD.

SINR region.

The RL channels are projected over the $\mathbf{F}(\theta_c)$ codebook and the spatial power spectrum is expressed by

$$\mathbf{P}(\theta_c) = \frac{1}{\mathbf{F}(\theta_c)^{\mathrm{H}}\mathbf{Q}^{-1}\mathbf{F}(\theta_c)}, \tag{2.12}$$

where $\mathbf{P}(\theta_c)$ is the spatial power spectrum, $\mathbf{Q} = \mathbf{H}_{ji}\mathbf{H}_{ji}^{\mathrm{H}}$ is the $N_t \times N_t$ auto-covariance matrix of the RL channel and $\mathbf{F}(\theta_c)$ is the $N_t \times 1$ steering vector from the codebook that corresponds to the direction angle θ_c. The N_t angles that correspond to the largest power values are considered the principal estimated FL AoDs and the AoD angle vector is estimated as

$$\hat{\boldsymbol{\theta}}_{AoD} = \left[\theta_{AoD_1}, \theta_{AoD_2}, \ldots, \theta_{AoD_{N_t}}\right]^{\mathrm{T}}, \tag{2.13}$$

$$\theta_{AoD_w} = \arg\max_{\theta_c} \left\|\mathbf{P}(\theta_c)\right\|^2, \forall w = 1, 2, \ldots, N_t. \tag{2.14}$$

A transformation matrix is constructed to roughly estimate the FL channel, where

the dominant N_t FL AoDs are known. The transformation matrix $\mathbf{T}(\theta_{AoD}) \in C^{N_t \times N_t}$ re-projects the RL channel column vectors on the estimated AoD directions,

$$\mathbf{T} = \begin{bmatrix} 1 & \cdots & 1 \\ e^{\psi \cos\theta_{AoD_1}} & \ddots & e^{\psi \cos\theta_{AoD_{N_t}}} \\ \vdots & \vdots & \vdots \\ e^{\psi(N_t-1)\cos\theta_{AoD_1}} & \cdots & e^{\psi(N_t-1)\cos\theta_{AoD_{N_t}}} \end{bmatrix} \tag{2.15}$$

where $\psi = -j2\pi\triangle_{\mathrm{DL}}$. A rough estimate of the FL channel between the $j^{th} - i^{th}$ transmitter-receiver pair is obtained by projecting the RL channel on the transformation matrix $\mathbf{T}$ as

$$\hat{\mathbf{H}}_{ij} = \mathbf{H}_{ji}^{\mathrm{H}}\mathbf{T}. \tag{2.16}$$

Based on (2.13)-(2.16), it can be easily seen that with an increased number of transmit antennas, additional spatial information of the RL channel is captured and the beamforming directions from the codebook become sharper, leading to less interference on the spatial power spectrum. Thus, the estimation accuracy is improved without additional feedback bits as it will be shown in Section 2.5.

2.4.2 Minimum Mean Squared Estimate of the FL Channel

The rough channel estimation obtained in (2.16) is refined by using the MMSE criterion. The estimation problem of the FL channel is given by

$$\hat{\mathbf{H}}_{ij} = \mathbf{H}_{ji}^{\mathrm{H}}\mathbf{T} + \boldsymbol{G}, \tag{2.17}$$

where $\mathbf{G} \in C^{M_r \times N_t}$ is the estimation Gaussian error covariance matrix. The MMSE approach finds the matrix $\mathbf{W}$ which minimizes the MSE as expressed by

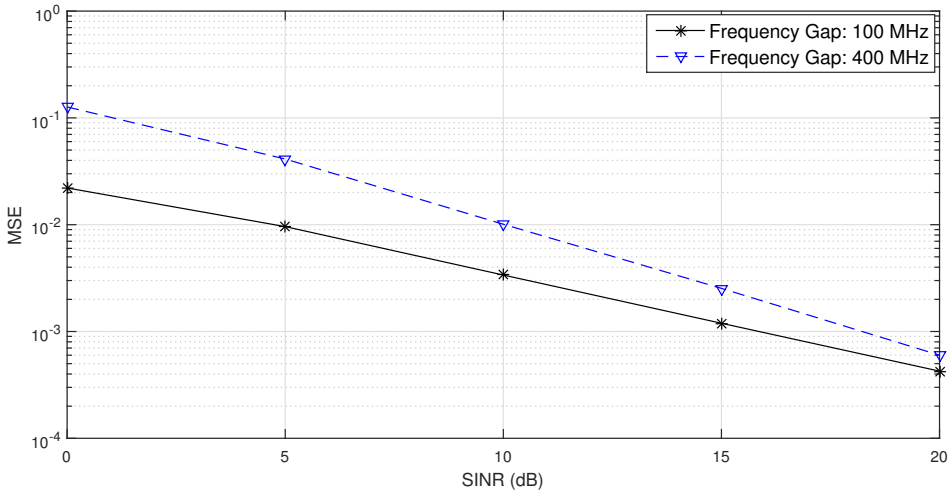

Figure 2.3: MSE for different frequency gaps.

$$\text{MSE} = \mathbb{E}\left\{(\mathbf{W}\mathbf{H}_{ji}^{\text{H}}\mathbf{T} - \mathbf{H}_{ij})(\mathbf{W}\mathbf{H}_{ji}^{\text{H}}\mathbf{T} - \mathbf{H}_{ij})^{\text{H}}\right\}, \tag{2.18}$$

where $\mathbb{E}\{.\}$ denotes the expectation and $\mathbf{H}_{ij}$ is the actual FL channel. Hence, the $\mathbf{W}$ matrix is given by $\mathbf{W} = ((\mathbf{H}_{ji}^{\text{H}}\mathbf{T})^{\text{H}}\mathbf{H}_{ji}^{\text{H}}\mathbf{T} + \sigma_G^2\mathbf{I})^{-1}(\mathbf{H}_{ji}\mathbf{H}_{ji}^{\text{H}}\mathbf{T})^{\text{H}}$, and the final channel estimate is given by $\hat{\mathbf{H}}_{ij} = \mathbf{W}\mathbf{H}_{ji}^{\text{H}}\mathbf{T}$. The MSE of the proposed SCEIA estimator is shown in Figure 2.3; as noticed, the MSE converges to a small arbitrary error value with the SINR, regardless of the frequency gap.

2.5 Simulation Results

The 3GPP SCM channel is used with uniform linear antenna array, and each node desires to accommodate $d_i = 2$ independent streams with the maximum likelihood detection.

Figure 2.4 compares the bit error rate (BER) performance under three different cases, namely perfect channel reciprocity, proposed SCEIA method and the case without frequency compensation between channels. The proposed method shows sig-

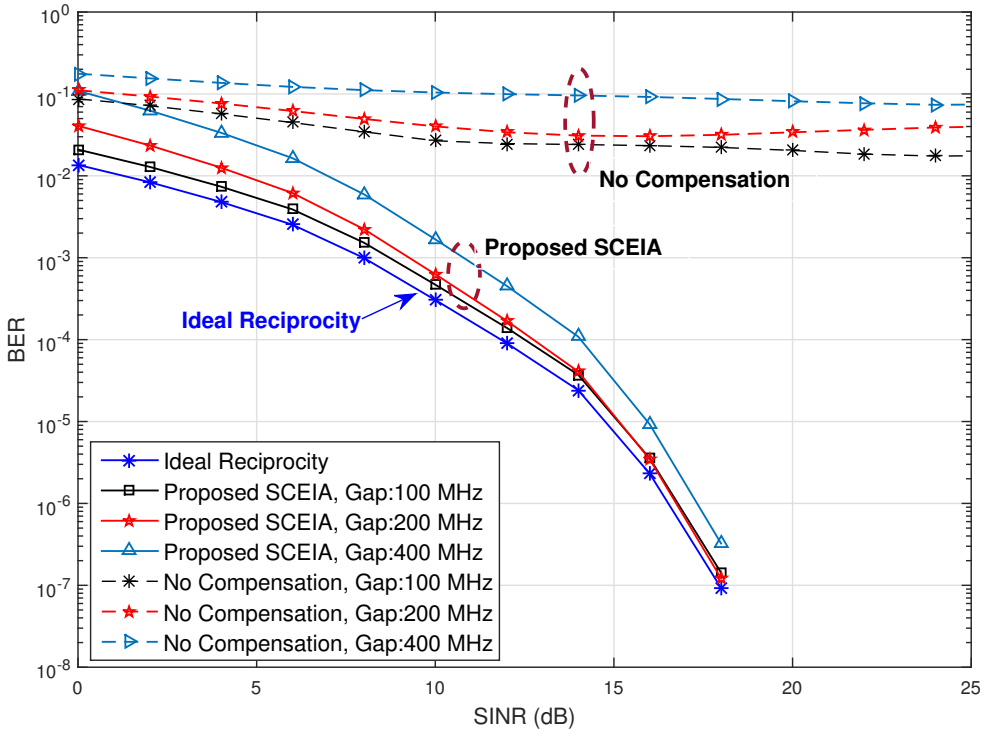

Figure 2.4: BER performance of the SCEIA with 4×4 MIMO channel.

nificant performance improvement, and approaches the ideal case of perfect channel reciprocity at high SINR. With different frequency gaps between the RL and FL channels, the IA without channel compensation suffers from severe performance degradation due to the channel path mismatch. Therefore, the maximum SINR algorithm is misled by inaccurate channels and results in non-aligned interference at the receivers. The IA DoFs are accordingly lost.

In Figure 2.5, the sum rate (SR) performance in bits/sec/Hz is shown for the same three cases. Similar observations are concluded. When there is no compensation for the channels under different frequency gaps, the SR saturates under 18 bits/sec/Hz. The proposed SCEIA method shows linear SR gain with the SINR, since the overall interference is properly confined in one signal subspace by the IA maximum SINR criterion with the estimated channels. It is worth noting that a similar behavior is

observed with the zero-forcing detector; these results are not included due to space limitation.

Additionally, we compare the SR performance of the proposed SCEIA method with the proposed work in [10]. Authors in [10] proposed a quantized-precoder based IA (QP-IA), where only the receive decoders are designed by using non-quantized vectors as a tradeoff between the overall quantization error and size of the feedback bits. Once the precoders are obtained, they are quantized by using a predefined codebook $\mathbf{C} = \{\boldsymbol{c}_1, \boldsymbol{c}_2, \ldots, \boldsymbol{c}_{2^B}\}$, where each codeword is represented by a B-bit index. Then, the quantized precoders are selected based on the minimization of the chordal distance. However, a large number of feedback bits is still required to enhance the quantization accuracy, e.g., B = 12 or 20 bits. Figure 2.5. shows that the proposed SCEIA method provides improved system SR without the cost of additional feedback bits, since no FL channel quantization is needed. The QP-IA method suffers from SR degradation, as the FL channel quantization precision is always limited by the size of the codebook. Therefore, larger codebooks are needed.

Moreover, the performance gain of SCEIA is shown to be enhanced with the number of transmit antennas as in Table 2.1. With larger N_t, it enables capturing additional spatial information about the estimated FL channel AoDs.

2.6 Conclusion

In this chapter, a spatial channel estimation method for FDD-MIMO IA systems (SCEIA) has been proposed. SCEIA utilized the fact that the reverse and forward spatial channel clusters bounce on similar sub-paths with a given frequency gap between channels. The SCEIA method exhibited a significant performance gain. This gain is shown to improve as the number of transmit antennas increases, making it ap-

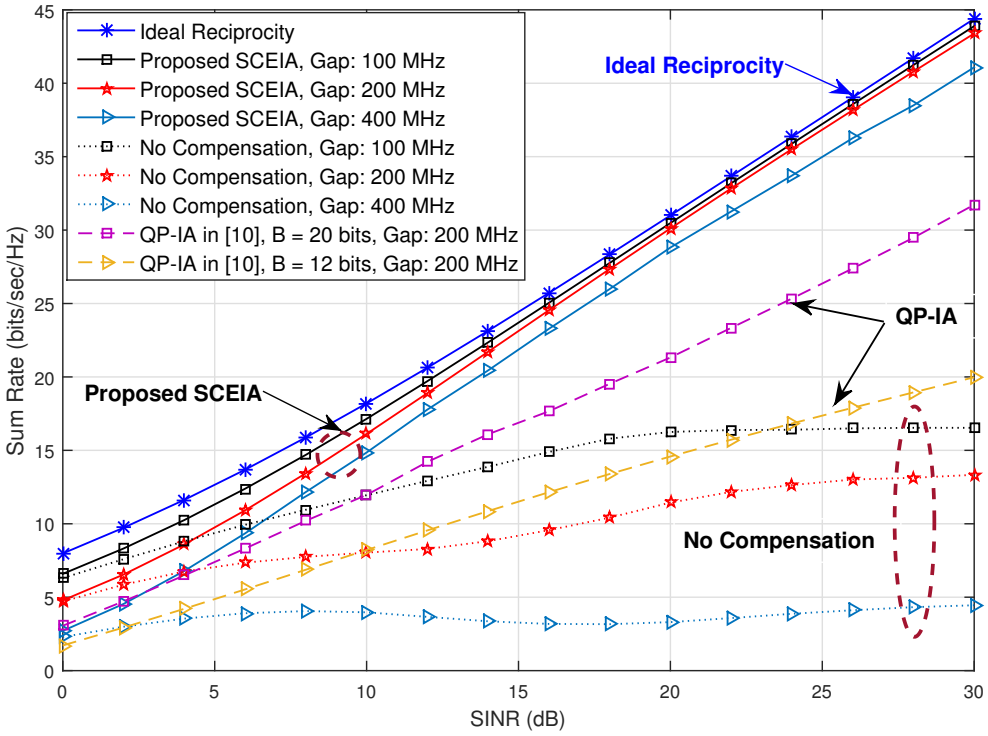

Figure 2.5: Sum rate performance of the SCEIA with 4×4 MIMO channel.

Table 2.1: Estimation Precision for Different Tx Antenna Number.

	2×2		8×2	
	Ideal	Gap: 200 MHz	Ideal	Gap: 200 MHz
SR (b/s/Hz)	16.06	12.95	29.17	27.60
Loss (%)	0.00	21.3	0.00	5.5

propriate for future massive MIMO systems. A detailed study under such a scenario will be performed in future work.

References

[1] M. El-Absi, "Novel Aspects of Interference Alignment in Wireless Communications," PhD. thesis, Duisburg-Essen Univ., Germany, 2015.

[2] N. Zhao, F. R. Yu, M. Jin, Q. Yan, and V. C. M. Leung, "Interference Alignment

and Its Applications", Research Issues, and Challenges," *IEEE Commun. Soc. Mag.*, vol. 18, no. 3, pp. 1779-1803, Mar. 2016.

[3] V. R. Cadambe, S. A. Jafar, and S. Shamai, "Interference Alignment on the Deterministic Channel and Application to Fully Connected Gaussian Interference Networks," *IEEE Trans. Inform. Theory.*, vol. 55, no. 1, pp. 269-274, Jan. 2009.

[4] X. Rao and V. K. N. Lau, "Minimization of CSI Feedback Dimension for Interference Alignment in MIMO Interference Multicast Networks," *IEEE Trans. Inform. Theory.*, vol. 61, no. 3, pp. 1218-1246, Mar. 2015.

[5] A. Jafar, *Interference Alignment — A New Look at Signal Dimensions in a Communication Network*. Boston: Foundations and Trends in Communications and Information Theory, 2011.

[6] O. El Ayach and R. W. Heath, "Grassmannian Differential Limited Feedback for Interference Alignment," *IEEE Trans. Signal Process.*, vol. 60, no. 12, pp. 6481-6494, Apr. 2012.

[7] S. M. Razavi and T. Ratnarajah, "Performance Analysis of Interference Alignment Under CSI Mismatch," *IEEE Trans. Veh. Technol.*, vol. 63, no. 9, pp. 4740-4748, Nov. 2014.

[8] H. Huang, V. Lau, Y. Du, and S. Liu, "Robust Lattice Alignment for MIMO Interference Channels With Imperfect Channel Knowledge," *IEEE Trans. Signal Process.*, vol. 59, no. 7, pp. 3315-3325, July 2011.

[9] M. Rezaee and M. Guillaud, "Limited Feedback for Interference Alignment in the K-user MIMO Interference Channel," in *Proc. IEEE ITW*, Lausanne, 2012, pp. 667-671

[10] M. Kim, H. Lee, and Y. Ko, "Limited Feedback Design for Interference Alignment on Two-Cell Interfering MIMO-MAC," *IEEE Trans. Veh. Technol.*, vol. 64, no. 9, pp. 4019-4030, Sep. 2015.

[11] Spatial Channel Model for Multiple Input Multiple Output (MIMO) Simulations (Release 11), 3GPP, TR 25.996 V11.0.0, Sep. 2012.

[12] H. Xie, F. Gao, S. Zhang, and S. Jin, "A Unified Transmission Strategy for massive MIMO Systems with Spatial Basis Expansion Model," *IEEE Trans. Veh. Technol.*, vol. PP, no. 99, pp. 1-14, Mar. 2016.

Chapter 3

Blind Spatial Channel Estimation for Massive MIMO Systems *

3.1 Abstract

Channel state information (CSI) acquisition is a crucial issue in downlink FDD-based massive multi-input multi-output (MIMO) networks, where the channel reciprocity is not applicable. Thus, users are expected to feedback the best-match quantized channels to serving transmitters. Hence, an extensively large size of the feedback overhead is needed, which scales lineraly at each user with the number of transmit antennas at the base-station (BS). In turn, the uplink (UL) channel capacity may be consumed and the overall performance becomes fundamentally limited by the downlink (DL) channel quantization precision. An alternative CSI acquisition scheme is critically needed. In this chapter, we propose a novel FDD massive MIMO system based on a spatial DL channel estimation scheme; it relies on the statistical spatial correlation of

*This chapter is a modified version of "Ali A. Esswie, Mohammed El-Absi, Octavia A. Dobre, Salama Ikki and Thomas Kaiser, "A novel FDD massive MIMO system based on downlink spatial channel estimation without CSIT," in *Proc. IEEE ICC*, Paris, 2017, pp. 1-6."

the UL and DL channel clusters, given an arbitrary frequency band gap between the UL and DL channels. A transformation matrix is constructed to precode the observed UL channel on the estimated dominant DL angles of departure. The proposed scheme significantly outperforms the recent state-of-the-art techniques, without the cost of user feedback overhead bits and prior knowledge of the channel statistics.

Index Terms— Massive MIMO; Reciprocity; 5G; Channel state information; Feedback; Estimation.

3.2 Introduction

Massive multi-input multi-output (MIMO) has been considered in the recent years as one of the key techniques towards the fifth generation (5G) networks [1]. With larger transmit antenna arrays, the channel hardening phenomenon becomes more prominent to cancel the channel small-scale fading characteristics. As a result, the massive MIMO channel tends to be a set of orthogonal sub-channels with almost scalar and frequency-independent gains [2]. Hence, massive MIMO communication can dramatically improve the overall spectral efficiency and user capacity with simple linear transmit and receive filters. Moreover, many promising techniques towards 5G have been recently proposed such as interference alignment (IA) [3] and spatial modulation (SM) [4], which completely rely on the spatial degrees of freedom (DoFs) provided by the large antenna arrays, that in turn push the motivation toward the feasibility of the massive MIMO systems.

Frequency division duplex (FDD) networks are widely employed in current standards because they offer different advantages over time division duplex (TDD), e.g., smaller latency and continuous channel estimation [5]. Unfortunately, harvesting the potential gains of an FDD-based massive MIMO system requires perfect channel state

information at the transmitter (CSIT), which is linearly scaled with the number of transmit antennas to limit the quantization error [5]. In this way, the downlink (DL) training pilots to acquire the CSIT overwhelm the DL channel capacity and the user feedback overhead bits accordingly consume the uplink (UL) channel. A straightforward solution to overcome this issue is to employ a TDD system and exploit the channel reciprocity through the UL training. However, perfect channel reciprocity does not strictly hold even with TDD communication due to the radio chain calibration error [6]. Additionally, when the number of served users significantly increases, the performance of the TDD-based massive MIMO systems becomes limited by the corresponding increase in the UL training reuse rate [7].

Studies in the literature exploited perfect channel reciprocity, which is not suitable for FDD systems [7]. For FDD networks, research works traded feedback overhead with quantization performance. Authors in [8] proposed an alternative CSI acquisition method to spatially infer the DL covariance matrix from the observed UL covariance matrix. A recent work [9] found that lower-dimension overhead training pilots based on correlated massive MIMO channels are feasible in practice. Other studies exploited the spatial correlation of the massive MIMO channels in dense networks to scale the training overhead with the virtual antenna ports instead of the physical antennas by using either random beamforming [10] or the users clustered spatial signatures, which are greatly lower than the the number of transmit antennas [11].

Compared to the majority of the existing research, some studies exploit the pre-existing knowledge of partial information about channel statistics, which may not be always feasible in practice [9]. Other works require very large quantization codebooks to achieve near-perfect-CSI performance [12], which accordingly leads to severe loss in the overall sum rate due to the large user feedback overhead, e.g., 20 bits per user. Needless to say that a CSI acquisition scheme, which effectively minimizes

the feedback overhead with minimal impact on the overall performance, is crucial to achieve the potential gains of the FDD-based massive MIMO networks.

In this chapter, we propose an FDD massive MIMO system based on DL spatial channel estimation (FMMSCE). The FMMSCE scheme is valid for FDD communications under any arbitrary frequency band difference. It requires neither DL overhead training pilots nor UL user feedback overhead bits. FMMSCE projects the UL channel, known from the UL sounding, on a set of beamforming directions, which compose a predefined codebook that spans the entire coverage space of the antenna sector. The beamforming vectors in the codebook are compensated by the frequency band gap between the UL and DL channels. The spatial power spectrum is drawn and a vector of the principal DL angles of departure (AoDs) is estimated. Finally, a beamforming matrix is constructed to estimate the DL channel. Thus, the overall performance of the FDD-based massive MIMO systems can be fundamentally relieved from the bottleneck of the DL channel quantization accuracy. The proposed scheme is generally valid in outdoor urban environments with the spatial channel modeling. The advantages of the FMMSCE scheme over the state-of-the-art schemes are as follows:

- Unlike [8, 9, 10, 11, 18], FMMSCE requires no user feedback overhead bits in the UL direction, with better estimation performance.

- FMMSCE can be easily implemented using the fast Fourier transform (FFT) without the cost of complex operations, e.g., singular and eigen value decomposition operations (SVD and EVD) [19].

This chapter is organized as follows. Section 3.3 introduces the system model. Section 3.4 presents the FMMSCE scheme. Performance results are discussed in Section 3.5 and conclusion is drawn in Section 3.6.

3.3 System Model

We consider a DL multi-user massive MIMO system, where a base station (BS) is equipped with N transmit antennas and K randomly distributed users with M receive antennas. The k^{th} user desires to accommodate M independent data streams $s_k = \boldsymbol{\mathcal{CN}}(0, \frac{P}{M}\mathbf{I}_M)$. The DL channel from the BS to the k^{th} user is denoted by $\mathbf{H}_k \in C^{M\times N}, \forall k \in \{1, 2, \ldots, K\}$.

The received signal at the k^{th} user is described by

$$\boldsymbol{y}_k = \mathbf{H}_k\mathbf{U}_k\mathbf{s}_k + \sum_{j=1,j\neq k}^{K} \mathbf{H}_j\mathbf{U}_j\mathbf{s}_j + \mathbf{n}_{\boldsymbol{k}}, \tag{3.1}$$

where $\mathbf{U}_k \in C^{N\times M}$ is the unit-norm precoding matrix, and $\mathbf{n}_k$ is the additive white Gaussian noise at the k^{th} user, respectively. The summation term represents the inter-user interference. For the beamforming vectors, we adopt zero-forcing beamforming (ZFBF) where precoders are expressed by the pseudo inverse of the DL channels as $\mathbf{U}_{\mathrm{zf},k} = \mathbf{H}_{\boldsymbol{k}}{}^{\mathrm{H}}(\mathbf{H}_{\boldsymbol{k}}\mathbf{H}_{\boldsymbol{k}}{}^{\mathrm{H}})^{-1}$.

The sum rate is given by [5]

$$\mathit{F} = \sum_{k=1}^{K} \log_2\left(1 + \frac{\frac{P}{K} \mid \mathbf{H}_k\mathbf{U}_k \mid^2}{1 + \frac{P}{K}\sum_{j=1,j\neq k}^{K} \mid \mathbf{H}_j\mathbf{U}_j \mid^2}\right), \tag{3.2}$$

where $|.|$ denotes the matrix determinant. The 3GPP spatial channel model (SCM) is adopted in this work [13], to reflect the spatial channel correlation due to the scatters. The channel model is expressed by

$$\mathbf{H}_k = \mathbf{A}_k\beta_k^{0.5}, \qquad k = 1, 2, \ldots K, \tag{3.3}$$

where $\beta_k = \phi w_k^{\alpha}\xi_k$ is the large-scale coefficient, ϕ is a constant in terms of the antenna gain and operating frequency, w_k is the distance between the BS and the k^{th} user, α

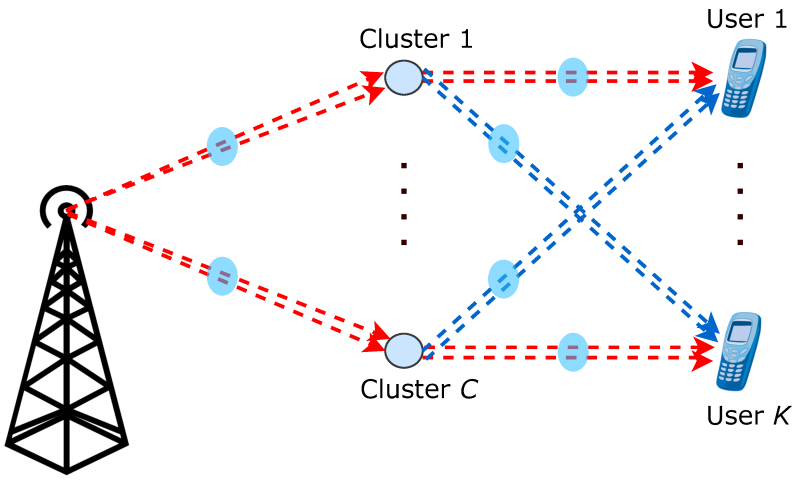

Figure 3.1: The 3GPP spatial channel modeling.

is the path loss exponent, and ξ_k is the log shadow fading. The block-fading channel at the k^{th} user is expressed as

$$\mathbf{A}_k = \mathbf{R}_k \mathbf{G}_k, \tag{3.4}$$

where $\mathbf{G}_k = \boldsymbol{\mathcal{CN}}(0,1)$ and the steering matrix $\mathbf{R}_k \in C^{M \times N}$ contains the correlated spatial characteristics of the channel. In 3GPP standards [13], the SCM is described by the strongest $C = 6$ clusters, each with 20 rays, as shown in Figure 3.1. The steering element $R_{(m,n,c)_k}$ from the transmitting n^{th} to the receiving m^{th} antenna on the c^{th} channel cluster towards the k^{th} user is given by

$$R_{(m,n,c)_k} = \sqrt{\tfrac{\mu_c \sigma}{20}} \sum_{z=1}^{20} \left(\sqrt{g_T(\theta_{c,z,\mathrm{AoD}})} e^{j[\zeta \varepsilon \sin(\theta_{c,z,\mathrm{AoD}})]}\right)$$

$$\times \left(\sqrt{g_R(\theta_{c,z,\mathrm{AoA}})} e^{j[\zeta \epsilon \sin(\theta_{c,z,\mathrm{AoA}})]} e^{j\zeta ||v|| cos(\theta_{c,z,\mathrm{AoA}} - \theta_v)t}\right), \tag{3.5}$$

where μ_c and σ are the power and shadow fading coefficient of the c^{th} cluster, g_T and g_R are the BS and user antenna gains respectively, ζ is the wave number where $\zeta = \frac{2\pi}{\lambda}$ and λ is the carrier wavelength, $\theta_{c,z,\mathrm{AoD}}$ and $\theta_{c,z,\mathrm{AoA}}$ are the DL AoD and UL AoA

respectively, ε is the distance in meters between the n^{th} antenna and the reference antenna index, and v is the relative velocity between the BS and the k^{th} user.

3.4 FDD massive MIMO System based on Downlink Spatial Channel Estimation

The FMMSCE scheme exploits the statistical phase correlation of the large antenna array based on a novel DL spatial channel estimation scheme without CSIT. A predefined codebook, which contains Q beamforming channel directions, is created at the BS to span the entire angular space of the antenna sector; the codebook design, e.g., beam separation angle is arbitrary for a given quantization accuracy [14]. The observed UL channel per user is projected on the angular space of the codebook and finally the spatial power spectrum is obtained. The dominant DL AoDs are estimated in terms of the frequency band gap. The DL channel is estimated by precoding the UL channel in the directions of the estimated AoDs. The minimum mean square estimate (MMSE) of the DL channel is calculated to refine the estimation accuracy.

3.4.1 Uplink Channel Spatial Projection

Ideally, the DL and UL channel clusters bounce on correlated paths [13]. The path correlation between the UL and DL channels depends on the frequency band gap Ω. Hence, with larger values of Ω, the dominant UL AoAs and DL AoDs deviate from each other, leading to employing very large codebooks to fully acquire CSIT. Figure 3.2. shows the angular deviation between the dominant UL AoAs and DL AoDs of a randomly selected user as Ω increases, e.g., 100, and 200 MHz, respectively. It shows that the assumption of perfect channel reciprocity does not even hold with $\Omega = 0$ MHz [6] and the angle deviation increases with Ω. Hence, the DL channel to the m^{th}

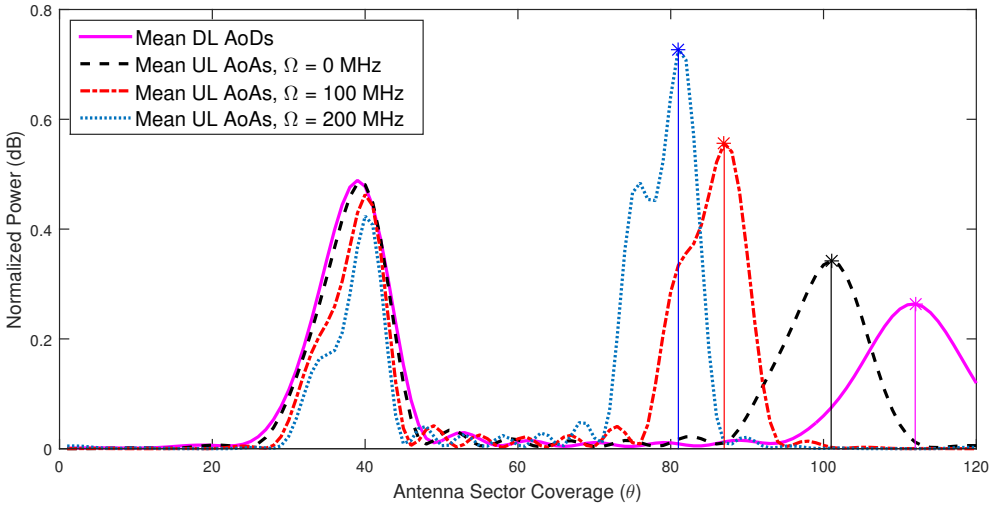

Figure 3.2: DL and UL spatial power spectra

receiving antenna at the k^{th} user can be represented by the lower-dimensional space of major channel clusters as,

$$\mathbf{h}_k^m = \frac{g_1^{\mathrm{dl}}}{\sqrt{N}} \begin{pmatrix} 1 \\ e^{\Psi_2 \cos\theta_1} \\ \vdots \\ e^{\Psi_2 \cos\theta_1} \end{pmatrix} + \ldots + \frac{g_C^{\mathrm{dl}}}{\sqrt{N}} \begin{pmatrix} 1 \\ e^{\Psi_N \cos\theta_C} \\ \vdots \\ e^{\Psi_N \cos\theta_C} \end{pmatrix}, \tag{3.6}$$

where $\Psi_x = -j\pi(x-1)$, $x = 2, 3, \ldots, N$, g_C^{dl} is the path gain of the DL channel corresponding to C^{th} cluster, $C = 6$ is the number of the major SCM clusters, $\theta_C = \theta_{\mathrm{AoD}_C} + \varphi_C$, θ_{AoD_C} is the AoD of the DL channel corresponding to C^{th} cluster and φ_C is a random angular deviation. Similarly, the UL channel from the k^{th} user to the n^{th} receiving antenna at the BS is expressed as $\overleftarrow{\mathbf{h}}_k^n = \sum_{r=1}^{C} g_r^{\mathrm{ul}} \boldsymbol{a}(\theta_r)$, where $\boldsymbol{a}(\theta_r) = \frac{1}{\sqrt{M}} \left[1, e^{-j\pi\cos\theta_r}, \ldots, e^{-j\pi(M-1)\cos\theta_r}\right]^{\mathrm{T}}$ is a steering vector in the direction of θ_r, the superscript T denotes the transpose operation. As the signal-to-noise- ratio (SNR) increases, the UL and DL channel gains are averaged over a fewer number of major channel clusters, e.g., two channel directions as in Fig. 2; thus, the average gain of

the principal UL and DL channel clusters tends to be a constant as

$$\frac{1}{N}\mathbb{E}\left\{\sum_{r=1}^{C} g_r^{(\mathrm{dl,ul})}\right\} = \Upsilon, \tag{3.7}$$

where $g_r^{(\mathrm{dl,ul})}$ is the DL or UL channel gain of the r^{th} cluster, and Υ is a constant. Based on these observations, we conclude that a simple compensation coefficient in the angular domain is required to estimate the dominant DL AoDs from the UL AoAs, given arbitrary Ω.

We consider an antenna coverage space of θ degrees and a predefined beamforming codebook of $Q = \frac{\theta}{\varrho}$ quantized channel directions, where ϱ is an integer scaling factor. Without loss of generality, we consider $\theta = 120^o$, $\varrho = 1$ and $Q = 120$. The beamforming codebook for $q = 1, 2, \ldots, Q$, is given by

$$\mathbf{W}(\theta_q) = \frac{1}{\sqrt{N}}\left[1, e^{-j2\pi\triangle_{\mathrm{UL}}\cos\theta_q}, \ldots, e^{-j2\pi\triangle_{\mathrm{UL}}(N-1)\cos\theta_q}\right]^{\mathrm{T}}, \tag{3.8}$$

where $\mathbf{W}(\theta_q)$ denotes the q^{th} beamformed channel direction from the codebook, which corresponds to the angular direction of θ_q and $\triangle_{\mathrm{UL}}$ is the effective antenna spacing after being compensated by the frequency band ratio as $\triangle_{\mathrm{UL}} = \gamma\triangle_{\mathrm{DL}}$, where $\gamma = \frac{f_{\mathrm{UL}}}{f_{\mathrm{DL}}}$ is the compensation coefficient, $\triangle_{\mathrm{DL}}$ is the actual DL antenna spacing in terms of the DL carrier frequency, and f_{DL} and f_{UL} are the DL and UL channel carrier frequencies, respectively. The compensation coefficient γ basically seeks to compensate for the angular difference between the major UL and DL channel clusters by the effective antenna spacing of the codebook directions, leading to adjusting the beam angular directions in the codebook, and hence, the spatial power spectrum based on the frequency gap Ω. With 64×2 antenna configuration, Figure 3.3 shows that the first estimated DL AoD approaches the actual AoD with a maximum mismatch of 1.5 degrees at SNR = 5 dB when employing the compensation coefficient γ, compared

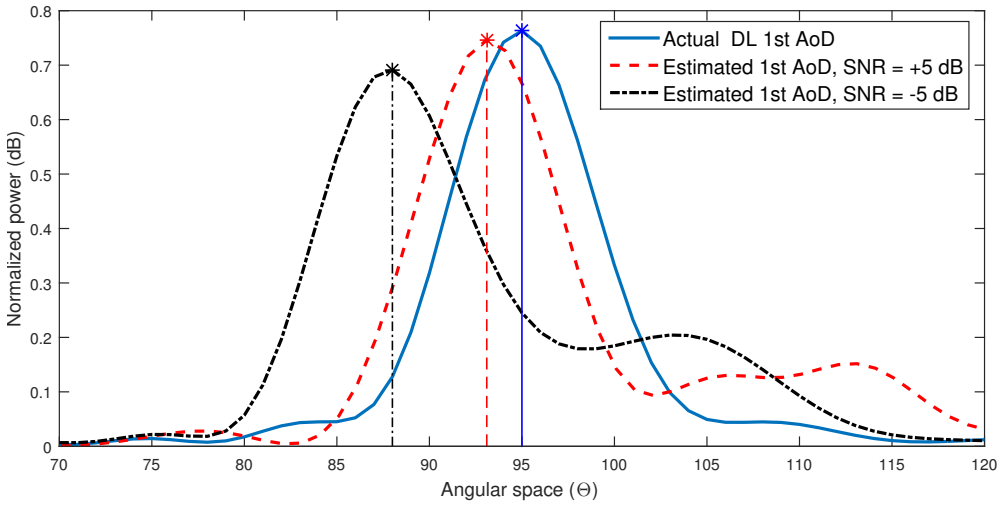

Figure 3.3: Spatial power spectra of the first DL AoD.

with an average mismatch of 22 degrees with Ω =100 MHz, as depicted in Figure 3.5.

The UL channel of the k^{th} user is spatially projected over the modified angular space of the $\mathbf{W}(\theta_q)$ codebook and the DL spatial power spectrum $\mathbf{P}(\theta_q)$ is given as

$$\mathbf{P}(\theta_q) = \left[\mathbf{W}(\theta_q)^{\mathrm{H}}\mathbf{D}^{-1}\mathbf{W}(\theta_q)\right]^{-1}, \tag{3.9}$$

where $\mathbf{D} = \overleftarrow{\mathbf{H}}_k\overleftarrow{\mathbf{H}}_k^{\mathrm{H}}$ is the $N \times N$ UL auto-covariance matrix, and $\overleftarrow{\mathbf{H}}_k$ is the UL channel of the k^{th} user. The N angular directions which correspond to the largest power values are considered the dominant estimated DL AoDs and the AoD angles are estimated as $\varphi_{\mathrm{AoD}_h} = \arg\max_{\theta_q} \|\mathbf{P}(\theta_q)\|^2, \forall h = 1, 2, \ldots, N$.

A beamforming matrix $\mathbf{V}(\theta_{\mathrm{AoD}}) = [\mathbf{v}_1, \mathbf{v}_2, \ldots, \mathbf{v}_N], \mathbf{v}_f \in C^{N\times 1}, \forall f \in \{1, 2, \ldots, N\}$ is constructed to obtain a rough estimate of the DL channel by precoding the observed UL channel clusters on the estimated N DL AoDs, where the beamforming vectors are given as : $\mathbf{v}_f = \left[1, e^{\psi\cos\varphi_{\mathrm{AoD}_f}}, \ldots, e^{\psi(N-1)\cos\varphi_{\mathrm{AoD}_f}}\right]^{\mathrm{T}}$, and $\psi = -j2\pi\triangle_{\mathrm{DL}}$. The rough estimate of the DL channel from the BS to the k^{th} user is obtained as

$$\hat{\mathbf{H}}_{k(1)} = \begin{bmatrix} \overleftarrow{h}_k^{1,1} & \cdots & \overleftarrow{h}_k^{1,M} \\ \vdots & \ddots & \vdots \\ \overleftarrow{h}_k^{N,1} & \cdots & \overleftarrow{h}_k^{N,M} \end{bmatrix}^{\mathrm{H}} \mathbf{V} = \overleftarrow{\mathbf{H}}_k^{\mathrm{H}} \mathbf{V}, \tag{3.10}$$

where $\overleftarrow{h}_k^{n,m}$ denotes the UL channel coefficient from the m^{th} antenna at the k^{th} user to the n^{th} antenna at the BS.

3.4.2 Minimum Mean Squared Estimate of the DL Channel

The DL channel channel estimate obtained in (3.10) is refined by the MMSE criterion. The estimation model is expressed as

$$\hat{\mathbf{H}}_k = \overleftarrow{\mathbf{H}}_k^{\mathrm{H}} \mathbf{V} + \mathrm{T}, \tag{3.11}$$

where $\mathbf{T} \in C^{M \times N}$ is the estimation Gaussian error. The MMSE criterion finds a filter $\boldsymbol{\mathcal{G}}$ to minimize the MSE as

$$\mathrm{MSE} = \mathbb{E}\left\{ (\boldsymbol{\mathcal{G}} \overleftarrow{\mathbf{H}}_k^{\mathrm{H}} \mathbf{V} - \mathbf{H}_k)(\boldsymbol{\mathcal{G}} \overleftarrow{\mathbf{H}}_k^{\mathrm{H}} \mathbf{V} - \mathbf{H}_k)^{\mathrm{H}} \right\}, \tag{3.12}$$

where $\mathbb{E}\{.\}$ denotes the statistical expectation. Thus, the $\boldsymbol{\mathcal{G}} = ((\overleftarrow{\mathbf{H}}_k^{\mathrm{H}} \mathbf{V})^{\mathrm{H}} \overleftarrow{\mathbf{H}}_k^{\mathrm{H}} \mathbf{V} + \sigma_{\mathrm{T}}^2 \mathbf{I})^{-1} (\overleftarrow{\mathbf{H}}_k \overleftarrow{\mathbf{H}}_k^{\mathrm{H}} \mathbf{V})^{\mathrm{H}}$, and the final estimate after MMSE is expressed as

$$\hat{\mathbf{H}}_{k(2)} = \boldsymbol{\mathcal{G}} \overleftarrow{\mathbf{H}}_k^{\mathrm{H}} \mathbf{V}. \tag{3.13}$$

For the 64×2 antenna setup, the MSE in (3.12) is displayed in Figure 3.4 for different values of Ω, results show that a small MSE is attained as SNR increases.

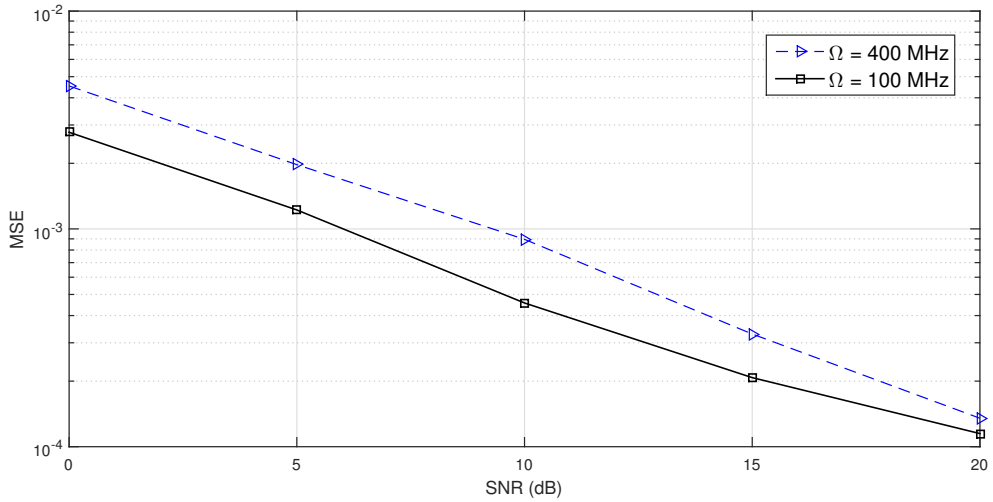

Figure 3.4: MSE of the FMMSCE estimator with Ω.

3.4.3 CSIT Feedback Overhead Comparison

Acquiring CSIT is vital in FDD networks. It becomes more challenging with the FDD massive MIMO communications, because the size of the user feedback overhead bits scales linearly with the number of transmit antennas [15, 16] as

$$\mathrm{B} = (N-1)\log_2 \mathrm{SNR}, \tag{3.14}$$

where B is the number of overhead bits per user, e.g., B = 424 bits for $N = 128$ antennas at SNR = 10 dB, which leads to significant loss in the UL resources.

In current LTE-advanced standards [17], dual 16-codeword codebooks for channel quantization are adopted to reduce the aggregate feedback overhead. It defines two different update rates (Λ_1, Λ_2) ms to select a codeword from each codebook, e.g., (5,5) ms means that each user feeds-back two $B = 4$-bit indices to select a codeword from each codebook every 5 ms.

Table 3.1 presents a comparison of the approximate average number of the user feedback bits to acquire CSIT and the overhead reduction gain (ORG), with respect

Table 3.1: CSIT Feedback Overhead: FMMSCE vs. Recent Works.

Scheme	Feedback (bits)	ORG
FMMSCE	0	100%
CCE [8] (Huawei)	33	67%
H-CSI [18] (Ericsson)	34	66%
SBEM [11]	60	40%
P-CSI [10] (Intel)	70	30%
Dual codebook (5,5) ms [17]	80	20%

to the optimal case in (3.14), between the FMMSCE and the recent state-of-the-art techniques from industry and academia, i.e., channel covariance estimation (CCE) [8], hybrid-CSI (H-CSI) [18], progressive-CSI (P-CSI) [10], and spatial basis expansion model (SBEM) [11]. To preserve fairness between all schemes, a unit time of $t_{\text{csit}} = 10$ CSI slots is adopted. The CCE builds a look-up channel dictionary between the observed UL channels and fed-back DL channels from all users over a variable period, e.g., initial $t_{\text{csit}} = 5$ slots. Over the rest, CCE does not require CSIT overhead, as it interpolates the channels from the dictionary. H-CSI and P-CSI scale the CSIT overhead with the virtual antenna ports. The SBEM divides the active cell users into τ clusters based on their spatial signatures, and the CSIT overhead is scaled with the number of the user clusters. The FMMSCE scheme shows significant reduction of the overhead bits with 100% ORG, since no DL quantization is employed.

On the other side, performance and overhead efficient schemes [19] adopt complex operations that are hardly practical to be implemented on micro processors, e.g., SVD and EVD of large-dimensional matrices. In contrast, the proposed FMMSCE scheme adopts a simple discrete Fourier transform (DFT) codebook. The estimated DL channel observed at the m^{th} receiving antenna of the k^{th} user $\overleftarrow{h}_k^m \in C^{1\times N}$ from (3.14) can be rewritten as

Table 3.2: Simulation Parameters of the Proposed FMMSCE.

Parameter	Value
Channel model	3GPP SCM-UMA
Channel bandwidth	10 MHz
BS antennas	64 Tx, 0.5λ
User antennas	2 Rx, 0.5λ
User dropping	Randomly distributed, 10 users/cell
User mobility	25 km/hr
Transmission mode	TM3, $M = 2$

$$\overleftarrow{h}_k^m = \left[\sum_{c=1}^{C} \left(g_c^{\text{ul}}\right)_1 e^{-j\theta_{\text{AoA},c,1}}, \ldots, \sum_{c=1}^{C} \left(g_c^{\text{ul}}\right)_N e^{-j\theta_{\text{AoA},c,N}}\right] \mathbf{V}, \tag{3.15}$$

where $\mathbf{V} = [\mathbf{v}_1, \mathbf{v}_2, \ldots, \mathbf{v}_N]$ is the DFT beamforming matrix, $\left(g_c^{\text{ul}}\right)_N$ and $e^{-j\theta_{\text{AoA},c,N}}$ are the average gain and AoA of the corresponding UL channel c^{th} cluster, respectively, observed on the N^{th} antenna at the BS. As noticed, the estimate $\overleftarrow{h}_k^m$ tends to be a sum of low-complexity shifted DFT operations.

3.5 Numerical Results

The 3GPP SCM channel is used with uniform linear antenna array at the BS and users for the 64×2 antenna setup. The detailed simulation parameters are listed in Table 3.2.

For the purpose of performance comparison, the following scenarios are considered in simulations:

1. **Perfect-CSIT**: the DL channel is assumed perfectly known without quantization at the BS.

2. **No conversion**: the DL channel is assumed to be fully reciprocal with UL channel, regardless of the frequency gap between UL and DL directions, e.g.,

$\mathbf{H}_k = \overleftarrow{\mathbf{H}}_k$.

3. **Conventional vector quantization** (CVQ): the conventional technique in literature to acquire the CSIT is by the DL channel quantization through a predefined codebook $\mathbf{C} = \{\boldsymbol{c}_1, \boldsymbol{c}_2, \ldots, \boldsymbol{c}_{2^B}\}$, where each codeword is represented by a B-bit index. Quantized channels $\hat{\boldsymbol{c}}$ are selected based on the minimization of the chordal distance, i.e., $\hat{\boldsymbol{c}} = \underset{c_b}{\arg\min}\{d^2(\boldsymbol{c}_b, \mathbf{H}_k)\}, \forall b = 1, 2, \ldots, 2^B$.

4. **Channel covariance estimation** (CCE) [8]: the CCE scheme [8] was shown to significantly reduce the CSIT feedback overhead by 67%, as in Table I. Initially, it requires full CSIT from all users during a training period. CCE builds a lookup channel dictionary between the observed UL channels and the fed-back quantized DL channels, e.g., ($\mathcal{U}_{DL}$,$\mathcal{U}_{UL}$). In the exploitation phase, CCE does not require CSIT feedback from users and when a new UL channel is observed, an interpolation on the Riemannian space is performed between the two least-distant DL channels from the dictionary to estimate $\mathcal{U}^{'}_{DL}$. Authors provided possible choices of the distance measures, e.g., the Euclidean distance.

Figure 3.5 presents the sum rate (SR) performance in bits/sec/Hz for the FMMSCE scheme and the previously mentioned schemes. The CVQ using a predefined codebook of size 512 quantized codewords, e.g., B = 9 bits, suffers from severe SR degradation due to the channel quantization error, which leads to losing the spatial DoFs provided by the large transmit antenna array. The CCE scheme provides a sub-optimal performance with an average SR loss of 35 bits/sec/Hz at SNR = 15 dB. To enhance the overall sum rate, CCE requires larger channel dictionaries in the training phase to enhance the interpolation precision with the cost of additional feedback overhead. The FMMSCE scheme clearly shows near perfect-CSIT SR, regardless of the frequency gap, e.g., Ω = 100, 400 MHz. The performance gains of the FMMSCE scheme are due

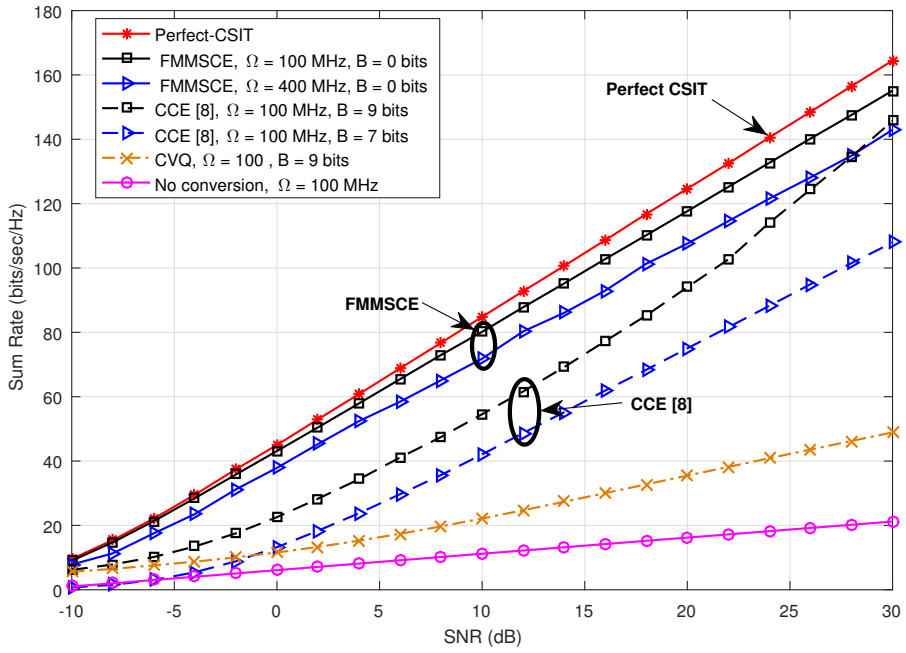

Figure 3.5: Sum rate performance of FMMSCE, compared with perfect-CSIT, CCE, CVQ and no conversion.

to the proper estimation of the principal DL AoDs with the compensation coefficient γ, removing the critical limitation of the DL channel quantization.

Similar conclusions can be observed from the BER performance with $\Omega = 100$ MHz, which is depicted in Figure 3.6. We compare the BER performance of the FMMSCE scheme with the previously mentioned schemes, i.e., no conversion, perfect-CSIT, CVQ and CCE. The FMMSCE scheme shows significant performance improvement over all schemes, approaching the perfect-CSIT case without CSIT overhead. It exhibits an average loss in the overall BER by a maximum of 1 dB with B = 0 bits, compared to 4 dB for the CCE scheme with B = 9 bits and 7 dB for the CVQ with B = 15 bits.

We define the DL channel quantization gain (CQG) η as a quality measure for the DL channel quantization accuracy as

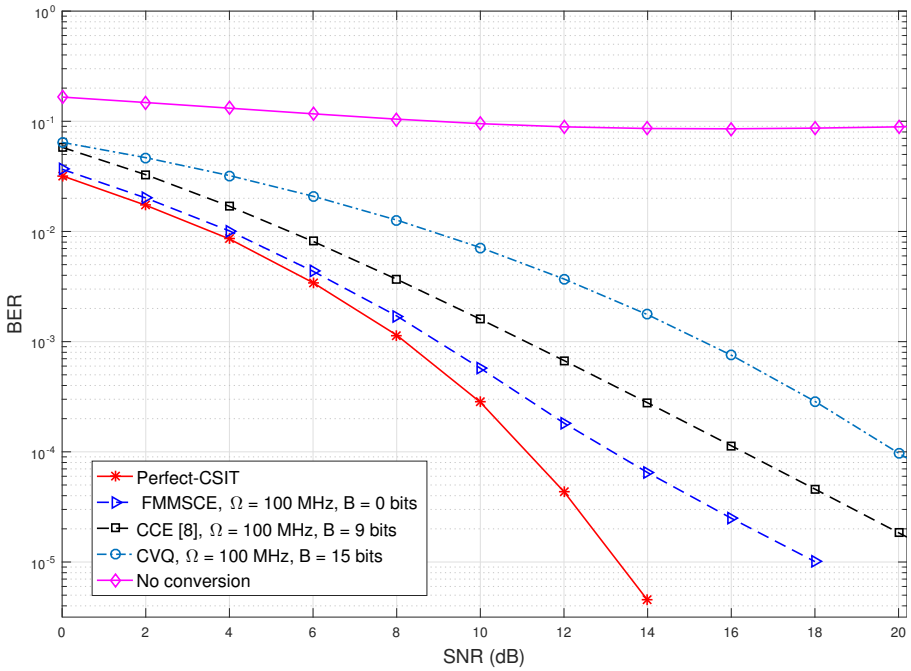

Figure 3.6: BER performance of FMMSCE, compared with perfect-CSIT, CCE, CVQ and no conversion.

$$\eta_k = \| \hat{\mathbf{H}}_b \times \mathbf{H}_k^{\mathrm{H}} \|^2, \quad b = 1, 2, \ldots, 2^B, \tag{3.16}$$

where $\hat{\mathbf{H}}_b$ is the quantized/estimated channel. Figure 3.7 compares the CQG of the FMMSCE scheme with respect to the perfect-CSIT, CCE and CVQ schemes. With perfect-CSIT, $\hat{\mathbf{H}}_b = \mathbf{H}_k$, and the CQG grows linearly with the number of transmit antennas, as shown in Figure 3.9. The CVQ scheme suffers from performance saturation when the number of transmit antennas exceeds the size of the DL codebook, leading to severe loss of the spatial DoFs. Larger codebooks may be needed with the cost of the CSIT overhead. The FMMSCE with B = 0 bits shows near perfect-CSIT CQG, outperforming both the CCE scheme with B = 9 bits and CVQ with B = 6, 5 bits, respectively. The FMMSCE scheme with the simple compensation coefficient for the channel angular deviation significantly reduces the distance between the estimated

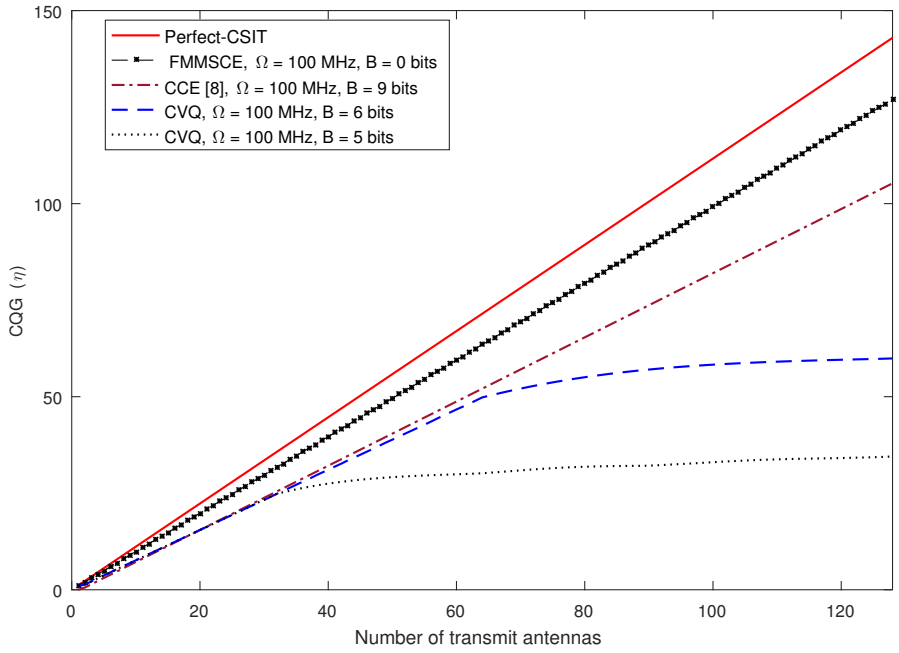

Figure 3.7: Quantization gain of the FMMSCE with N, compared with perfect-CSIT, CCE and CVQ.

and actual DL channels.

3.6 Conclusion

In this chapter, a novel FDD massive MIMO system based on a DL spatial channel estimation scheme (FMMSCE) has been proposed. The FMMSCE scheme utilizes the statistical phase correlation between the UL and DL channel clusters with an arbitrary frequency band gap. It exploits a simple compensation coefficient to efficiently estimate the DL channel without CSIT overhead. Compared with the recent state-of-the-art CSIT schemes, the FMMSCE scheme shows significant performance improvement, which approaches the perfect-CSIT. With simple implementation and zero CSIT overhead, this scheme relieves the FDD-based massive MIMO systems from the well known bottleneck of the DL channel quantization.

References

[1] T. L. Marzetta, “Noncooperative Cellular Wireless With Unlimited Numbers of Base Station Antennas,” *IEEE Trans. Wireless Commun.*, vol. 9, no. 11, pp. 3590–3600, Nov. 2010.

[2] T. L. Narasimhan and A. Chockalingam, "Channel Hardening-Exploiting Message Passing Receiver in Large-Scale MIMO Systems," *IEEE J. Sel. Topics Signal Process.*, vol. 8, no. 5, pp. 847-860, Oct. 2014.

[3] M. El-Absi, M. El-Hadidy, and T. Kaiser, “A Distributed Interference Alignment Algorithm Using Min-Maxing Strategy,” *Trans. Emerging Telecommun. Technol.*, Oct. 2014.

[4] A. Afana, T. M. N. Ngatched and O. A. Dobre, "Spatial Modulation in MIMO Limited-Feedback Spectrum-Sharing Systems With Mutual Interference and Channel Estimation Errors," *IEEE Commun. Lett.*, vol. 19, no. 10, pp. 1754-1757, Oct. 2015.

[5] D. J. Love, R. W. Heath Jr., V. K. N. Lau, D. Gesbert, B. D. Rao, and M. Andrews., “An Overview Of Limited Feedback In Wireless Communication Systems,” *IEEE J. Sel. Area Commun.*, vol. 26, no. 8, pp. 1341-1365, Oct. 2008.

[6] E. Bjornson, J. Hoydis, M. Kountouris, and M. Debbah, “Massive MIMO Systems With Non-Ideal Hardware: Energy Efficiency, Estimation, and Capacity limits,” *IEEE Trans. Inf. Theory*, vol. 60, no. 11, pp. 7112-7139, Nov. 2014.

[7] C. Shepard, H. Yu, N. Anand, L. E. Li, T. L. Marzetta, R. Yang, and L. Zhong, “Argos: Practical Many-Antenna Base Stations,” *in Proc. ACM Mobicom Netw. Conf.*, 2012, pp. 53-64.

[8] A. Decurninge, M. Guillaud, and D. Slock, “Channel Covariance Estimation In massive MIMO Frequency Division Duplex Systems,” *in Proc. IEEE GLOBECOM*, San Diego, CA, 2015, pp. 1-6.

[9] A. Adhikary, J. Nam, J.-Y. Ahn, and G. Caire, “Joint Spatial Division and Multiplexing: The Large-Scale Array Regime,” *IEEE Trans. Inf. Theory*, vol. 59, no. 10, pp. 6441–6463, Oct. 2013.

[10] M. Sajadieh, A. Esswie, A. Fouda, H. Shirani-Mehr and D. Chatterjee, "Progressive Channel State Information For Advanced Multi-User MIMO In Next Generation Cellular Systems," *in Proc. IEEE WCNC*, Doha, 2016, pp. 1-6.

[11] H. Xie, F. Gao, S. Zhang and S. Jin, "A Unified Transmission Strategy for massive MIMO Systems with Spatial Basis Expansion Model," *IEEE Trans. Veh. Technol.*, vol. PP, no. 99, pp. 1-14, Mar. 2016.

[12] H. Wang, W. Wang, V. K. N. Lau, and Z. Zhang, "Hybrid Limited Feedback in 5G Cellular Systems With massive MIMO," *IEEE Systems Journal*, vol. PP, no. 99, pp. 1-12, Aug. 2015.

[13] Spatial Channel Model for Multiple Input Multiple Output (MIMO) Simulations (Release 11), 3GPP, TR 25.996 V11.0.0, Sep. 2012.

[14] A. Esswie, M. El-Absi, O. A. Dobre, S. Ikki, and T. Kaiser, “Spatial Channel Estimation Based FDD-MIMO Interference Alignment Systems,” *Accepted in IEEE Wireless Commun. Lett.*, Feb. 2017.

[15] C. K. Au-Yeung and D. J. Love, “On The Performance of Random Vector Quantization Limited Feedback Beamforming In a MISO System,” *IEEE Trans. Wireless Commun.*, vol. 6, no. 2, pp. 458-462, Feb. 2007.

[16] G. Caire and S. Shamai, “On The Achievable Throughput of a Multi-Antenna Gaussian Broadcast Channel,” *IEEE Trans. Inf. Theory*, vol. 49, no. 7, pp. 1691-1706, Jul. 2003

[17] Evolved Universal Terrestrial Radio Access (E-UTRA); Physical layer procedures (Release 12), 3GPP, TS 36.213 V12.4.0, Feb. 2015.

[18] S. Faxer, S. Bergman, and N. Wernersson, "A Codebook-Based Concept for Hybrid CSI Feedback in FDD massive MIMO Systems," *in Proc. IEEE VTC Spring*, 2016, pp. 1-6.

[19] X. Rao and V. K. Lau, “Distributed Compressive CSIT Estimation and Feedback For FDD Multi-User massive MIMO Systems,” *IEEE Trans. Signal Process.*, vol. 62, no. 12, pp. 3261–3271, June 2014.

Chapter 4

Directional Spatial Channel Estimation for 3D 5G Networks *

4.1 Abstract

Full-dimensional (FD) channel state information at transmitter (CSIT) has always been a major limitation of the spectral efficiency of cellular multi-input multi-output (MIMO) networks. This chapter proposes an FD-directional spatial channel estimation algorithm for frequency division duplex massive FD-MIMO systems. The proposed algorithm uses the statistical spatial correlation between the uplink (UL) and downlink (DL) channels of each user equipment. It spatially decomposes the UL channel into azimuthal and elevation dimensions to estimate the array principal receive responses. An FD spatial rotation matrix is constructed to estimate the corresponding transmit responses of the DL channel, in terms of the frequency band gap between the UL and DL channels. The proposed algorithm shows significantly

*This chapter is a modified version of "Ali A. Esswie, Octavia A. Dobre, and Salama Ikki, "Directional spatial channel estimation for massive FD-MIMO in next generation 5G networks," *to be submitted.*"

promising performance, approaching the ideal perfect-CSIT case without UL feedback overhead.

Index Terms— Full-dimensional MIMO; spatial correlation; frequency division duplex; 5G; massive MIMO; CSI.

4.2 Introduction

Full dimensional massive multi-input multi-output (FD-mMIMO) is a key technology for boosting the spectral efficiency (SE) of 5G cellular networks [1]. Performance improvement of FD-mMIMO systems is achieved by using adaptive transmission at the base-station (BS) over the FD cell space. However, the assumption of perfect FD channel state information at the transmitter (FD-CSIT) is vital for achieving optimality, which is not feasible in practice [2, 3].

Hence, typical CSIT acquisition algorithms in time division duplex systems reasonably assume channel reciprocity, where the downlink (DL) channel can be approximated by the transpose of the uplink (UL) channel. In frequency division duplex (FDD) systems, channel reciprocity is not applicable due to the frequency band offset Ω. Consequently, channel quantization and limited-feedback algorithms have been widely considered [4]. Current LTE-Pro standards [5] define double-codebooks for tracking the channels small- and large-scale variations. For FD-mMIMO systems, the double-codebooks are extended to scan the azimuthal and elevation dimensions, providing a Kronecker-product (KP) based beamforming algorithm [6].

However, channel quantization represents a major limitation of the network spatial degrees of freedom, regardless of the number of transmit antennas [7]. Hence, the design of the beamformed CSI-reference-signals (CSI-RS) is widely studied in recent standards [8, 9], where the DL pilots are distributed across several FD beamforming

directions. CSI-RS algorithms have shown scalability and performance improvement with limited feedback overhead; however, they may result in blind coverage spots if scanning precision is insufficient. Furthermore, an FDD mMIMO system based on DL spatial channel estimation (FMMSCE) [7] has been recently proposed, to remove the limitation of the channel quantization; though, it suffers from sub-optimal performance in FD systems due to the missing elevation degrees of freedom (DoFs).

In this work, a directional spatial channel estimation (D-SCE) algorithm is proposed for FDD FD-mMIMO systems. The UL channel, is spatially projected over the FD space of a pre-designed discrete Fourier transform (DFT) codebook. The FD spatial power spectrum of the UL channel is estimated to obtain the instantaneous receive response of the antenna array. The estimated array response is spatially rotated in terms of Ω to compensate for the spatial deviation of the principal DL channel clusters and thereby attain the corresponding transmit response. Finally, the UL channel is spatially beamformed towards the principal set of the estimated transmit responses. The minimum mean square error (MMSE) criterion is applied to refine the estimation accuracy. The proposed D-SCE algorithm shows promising SE improvement, without the requirement of channel quantization or feedback overhead.

This chapter is organized as follows. In Section 4.3, the spatial channel modeling is presented. Section 4.4 introduces the proposed D-SCE algorithm. Performance results are discussed in Section 4.5 and conclusions are drawn in Section 4.6.

Notations: $(x)^{\mathrm{T}}$, $(x)^{\mathrm{H}}$ and $(x)^{\text{-}1}$ denote the transpose, Hermitian, and inverse operations on x. $x \otimes y$ stands for the Kronecker product of x and y, while $\overline{x}$ and $|x|$ represent the mean and absolute value of x. $x \sim \mathbb{CN}(0, \sigma^2)$ denotes a complex Gaussian random variable with zero mean and variance σ^2, while $\{x\}$ indicates the set of possible x values. $x_\kappa, \kappa \in \{\mathrm{ul}, \mathrm{dl}\}$ denotes the link direction of x.

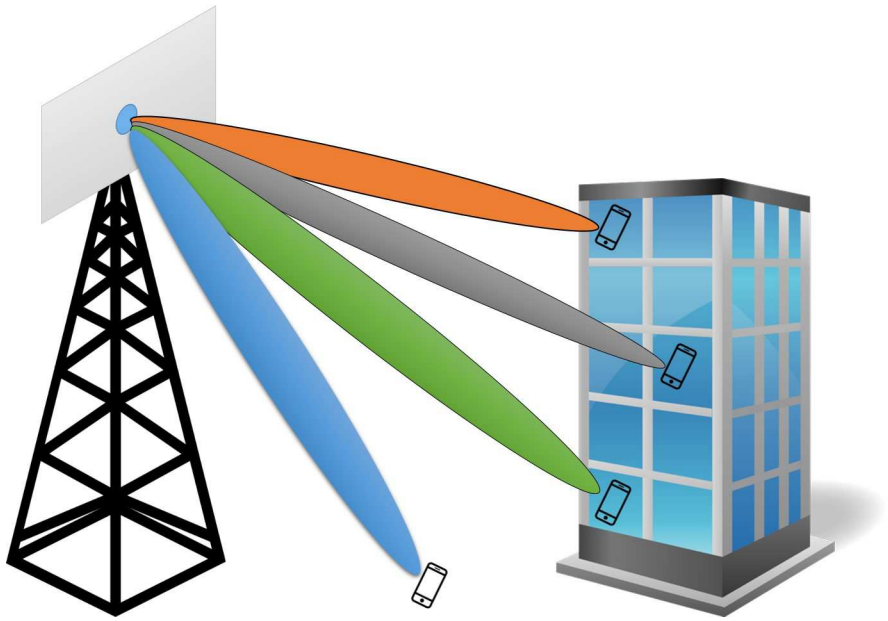

Figure 4.1: Full dimensional MIMO system model.

4.3 System Model

In this work, we consider a DL multi-user FD mMIMO system. A BS is mounted with $N_t = N_v \times N_h$ planar uniform rectangular array (URA), where N_v and N_h are the elevation and azimuthal antenna elements, respectively. There are K FD uniformly distributed users with M_r antennas, as shown in Figure 4.1. The received DL signal at the k^{th} user is expressed as

$$\boldsymbol{y}_k = \mathbf{H}_{\mathrm{dl},k}\mathbf{V}_k\mathbf{x}_k + \sum_{j=0,j\neq k}^{K-1} \mathbf{H}_{\mathrm{dl},j}\mathbf{V}_j\mathbf{x}_j + \mathbf{n}_{\boldsymbol{k}}, \tag{4.1}$$

where $\mathbf{H}_{\mathrm{dl},k} \in \mathbb{C}^{M_r \times N_t}, \forall k \in \{0, 1, \ldots, K-1\}$ is the DL spatial channel of the k^{th} user, $\mathbf{V}_k \in \mathbb{C}^{N_t \times 1}$ is the zero-forcing precoding matrix given as $\mathbf{V}_k = (\mathbf{H}_{\mathrm{dl},k})^{\mathrm{H}} \left(\mathbf{H}_{\mathrm{dl},k} (\mathbf{H}_{\mathrm{dl},k})^{\mathrm{H}}\right)^{-1}$, and $\mathbf{n}_{\boldsymbol{k}}$ is the additive white Gaussian noise. We adopt the spatially-correlated channel model [10], where the channel is described by its major C scattering clusters, spatially distributed over the FD cell space with Z rays per cluster. The DL channel coefficient from the n^{th} transmit antenna to the m^{th} receive antenna is given by

$$h_{(m,n)_k} = \frac{1}{\sqrt{C}} \sum_{c=0}^{C-1} \sqrt{\alpha_k}\, \mathcal{G}_{c,k}\, r_{(m,n,c)_k}, \tag{4.2}$$

where $\alpha_k = \ell \epsilon_k^{\beta} \mu_k$ is the channel large-scale factor, ℓ is a propagation constant, μ_k is the shadow fading factor, and ϵ_k^{β} is the separation distance, with β as the pathloss exponent, and $\mathcal{G}_{c,k} \sim \mathbb{CN}(0,1)$. The steering element $r_{(m,n,c)_k}$ of the channel coefficient is given by

$$r_{(m,n,c)_k} =$$

$$\sqrt{\frac{\xi\psi}{Z}} \sum_{z=0}^{Z-1} \begin{pmatrix} \sqrt{\mathfrak{D}_{\mathrm{BS}}^{m,n,c,z}(\theta_{\mathrm{AoD}}, \varphi_{\mathrm{EoD}})}\, e^{j(\eta d \overline{f} + \Phi_{m,n,c,z})} \\ \times \sqrt{\mathfrak{D}_{\mathrm{UE}}^{m,n,c,z}(\theta_{\mathrm{AoA}}, \varphi_{\mathrm{EoA}})}\, e^{j(\eta d \sin(\theta_{\mathrm{m,n,c,z,AoA}}))} \\ \times e^{j\eta ||s|| \cos(\varphi_{\mathrm{m,n,c,z,EoA}}) \cos(\theta_{\mathrm{m,n,c,z,AoA}} - \theta_s) t} \end{pmatrix}, \tag{4.3}$$

where ξ and ψ are the power and large-scale coefficient, $\mathfrak{D}_{\mathrm{BS}}^{m,n,c,z}$ and $\mathfrak{D}_{\mathrm{UE}}^{m,n,c,z}$ are the BS and UE spatial antenna patterns, η is the wave number, θ denotes the azimuthal angle of arrival θ_{AoA} and departure θ_{AoD}, while φ denotes the elevation angle of arrival φ_{EoA} and departure φ_{EoD}, respectively. s is the speed of the k^{th} user, $\overline{f} = f_x \cos\theta_{\mathrm{AoD}} \cos\varphi_{\mathrm{EoD}} + f_y \cos\varphi_{\mathrm{EoD}} \sin\theta_{\mathrm{AoD}} + f_z \sin\varphi_{\mathrm{EoD}}$ is the generic displacement vector of the transmit antenna array.

4.4 Proposed Directional Channel Estimation for FD-mMIMO Networks

4.4.1 Spatially-Correlated FD-MIMO Channels

The exact spatially-correlated FD-MIMO channel model, presented in Section 4.3, can be rewritten only by its predominant spatial clusters, distributed across the FD space of each antenna sector and with an average constant channel gain as

$$\mathbf{H}_{\kappa} = \frac{1}{\sqrt{C}} \sum_{c=0}^{C-1} g_{\kappa,c} \mathbf{a}_{\kappa,c}(\phi_c), \tag{4.4}$$

where $\mathbf{H}_{\kappa}, \kappa \in \{\text{ul}, \text{dl}\}$ is the UL/DL spatial channel matrix of an arbitrary user, $g_{\kappa,c}$ is the c^{th} cluster gain of the UL/DL channel, and $\mathbf{a}_{\kappa,c}(\phi_c)$ is the UL receive or DL transmit antenna FD response of the c^{th} cluster, with ϕ_c as the FD spatial angle of the corresponding antenna response. The FD antenna response $\mathbf{a}_{\kappa,c}(\phi_c)$ is composed of the horizontal and vertical responses by the Kronecker product as $\mathbf{a}_{\kappa,c}(\phi_c) = \mathbf{a}^h_{\kappa,c}(\theta_c) \otimes \mathbf{a}^v_{\kappa,c}(\varphi_c)$, where the horizontal $\mathbf{a}^h_{\kappa,c}(\theta_c)$ and vertical $\mathbf{a}^v_{\kappa,c}(\varphi_c)$ antenna response, in the azimuthal direction θ_c and elevation direction φ_c of the c^{th} cluster, are given by

$$\mathbf{a}^h_{\kappa,c}(\theta_c) = \left[1, e^{-j2\pi\Delta^h_{\kappa}\cos\theta_c}, \ldots, e^{-j2\pi\Delta^h_{\kappa}(N_h-1)\cos\theta_c}\right]^{\mathrm{T}}, \tag{4.5}$$

$$\mathbf{a}^v_{\kappa,c}(\varphi_c) = \left[1, e^{-j2\pi\Delta^v_{\kappa}\cos\varphi_c}, \ldots, e^{-j2\pi\Delta^v_{\kappa}(N_v-1)\cos\varphi_c}\right]^{\mathrm{T}}, \tag{4.6}$$

where Δ^h_{κ} and Δ^v_{κ} are the horizontal and vertical antenna physical spacing, respectively. The c^{th} FD cluster can be sampled in the DFT domain as

$$H_{\kappa,c}(b) = \sum_{n=0}^{N_t-1} g_{\kappa,c} e^{-j2\pi\Delta_{\kappa} n\cos(\phi_c)} e^{\frac{-j2\pi bn}{N_t}},\ b = 0, \ldots, N_t - 1, \tag{4.7}$$

where Δ_{κ} denotes the effective antenna spacing of the entire antenna array. The magnitude of $H_{\kappa,c}(b)$ is described by

$$|H_{\kappa,c}(b)| = |g_{\kappa,c}| \times \left| \frac{\sin\left(\frac{N_t}{2}\left(-2\pi\Delta_{\kappa}\sin\left(90-\phi_c\right) + \frac{2\pi}{N_t}b\right)\right)}{\sin\left(\frac{1}{2}\left(-2\pi\Delta_{\kappa}\sin\left(90-\phi_c\right) + \frac{2\pi}{N_t}b\right)\right)} \right|. \tag{4.8}$$

From (4.8), the leakage of each channel cluster becomes range-limited with the number of the transmit antennas. Hence, with large antenna arrays, the channel

dimension reduces to fewer and more predominant clusters. This leads to significant estimation precision if the directions of only the most predominant DL clusters are sufficiently approached. Furthermore, the c^{th} channel cluster gain is expressed as

$$g_{\kappa,c} = \Lambda_{\kappa,c}\gamma_{\kappa,c}\Upsilon_{\kappa,c}, \tag{4.9}$$

where $\Lambda_{\kappa,c}$ is a constant to represent the transmit power, and antenna gain. $\gamma_{\kappa,c}$ and $\Upsilon_{\kappa,c}$ are the large- and small-scale factors of the c^{th} channel cluster. In dense environments, where low mobility conditions are applicable, e.g., 30 km/h, the surrounding scatterers and Doppler shift slowly vary between two successive UL and DL transmissions of the same user. Thus, it is reasonable to assume that the average gain of both channel clusters is constant [10], being given as

$$\zeta = \frac{1}{N_t\sqrt{C}}\mathbb{E}\left(\sum_{c=0}^{C-1} g_{\kappa,c}\right), \tag{4.10}$$

where $\mathbb{E}$ denotes the statistical expectation. The optimal DL transmit response to maximize the received power of the c^{th} channel cluster is given by

$$\mathbf{a}_{\mathrm{dl},c}(\hat{\phi}_c) = \arg\max_{\phi}\left(\mathbf{a}^{\mathrm{H}}_{\mathrm{dl},c}(\phi)\,\mathbf{a}_{\mathrm{dl},c}(\phi_c)\,\mathbf{a}^{\mathrm{H}}_{\mathrm{dl},c}(\phi_c)\,\mathbf{a}_{\mathrm{dl},c}(\phi)\right), \tag{4.11}$$

where $\mathbf{a}_{\mathrm{dl},c}(\phi)$ and $\mathbf{a}_{\mathrm{dl},c}(\phi_c)$ are the estimated and actual DL transmit responses at the BS. Thus, the optimal transmit response $\mathbf{a}_{\mathrm{dl},c}(\hat{\phi}_c)$ should spatially align with the global set of the principal eigenvectors of the actual DL response $\mathbf{a}_{\mathrm{dl},c}(\phi_c)$, where $\hat{\phi}_c = \phi_c$. However, in FDD networks, the BS only accesses the UL receive response $\mathbf{a}_{\mathrm{ul},c}(\phi_c)$ since the transmit $\mathbf{a}_{\mathrm{dl},c}(\phi_c)$ and receive $\mathbf{a}_{\mathrm{ul},c}(\phi_c)$ antenna responses are not reciprocal, due to Ω. Furthermore, no closed-form relation between $\mathbf{a}_{\mathrm{dl},c}(\phi_c)$ and $\mathbf{a}_{\mathrm{ul},c}(\phi_c)$ exists in the literature, because it is a non-convex problem [5]. Hence, the knowledge of the actual DL transmit response $\mathbf{a}_{\mathrm{dl},c}(\phi_c)$ is not available at the BS. In

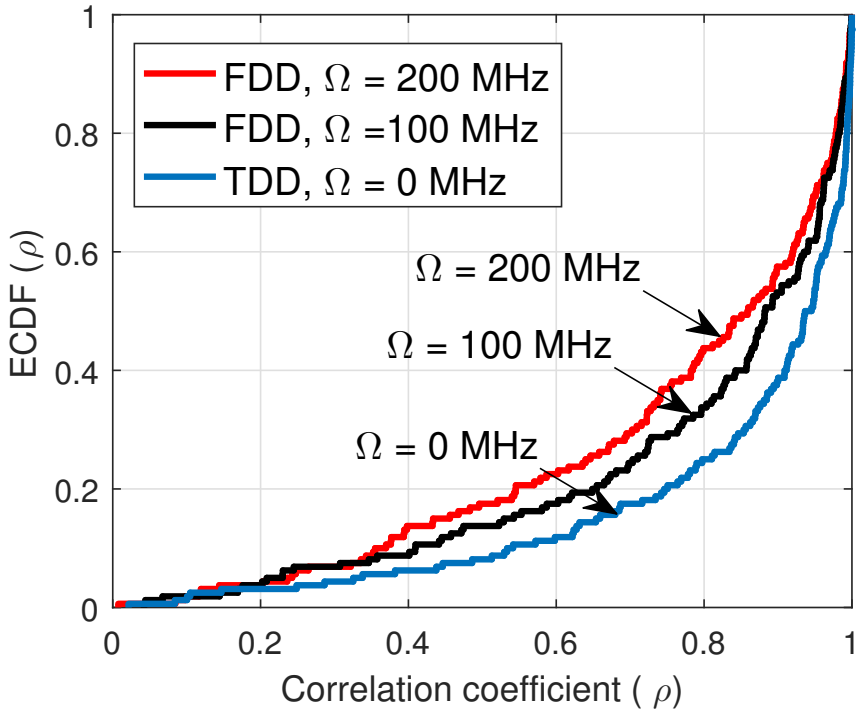

Figure 4.2: Empirical cumulative density function of the spatial correlation coefficient (ECDF (ρ)).

this work, we transform the optimization problem in (4.11), with the pre-knowledge requirement of the DL antenna response $\mathbf{a}_{\mathrm{dl},c}(\phi_c)$, into a search problem of the closest possible spatial directions, observed from the discrete spatial power spectrum of the UL channel, as it will be discussed subsequently.

Assuming a standard antenna sector of $120^o/90^o$ coverage in both the azimuthal and elevation directions, the FD cell space is spatially divided into U and Q elevation and azimuthal subspaces, with an arbitrary scanning precision. Then, we define an FD-DFT beamforming codebook at the BS to project the UL channel clusters over the virtual beamforming sub-spaces. An approximate estimate of the spatial power spectra of the UL/ DL channels, averaged over the C channel clusters within the entire FD space ϕ is given by

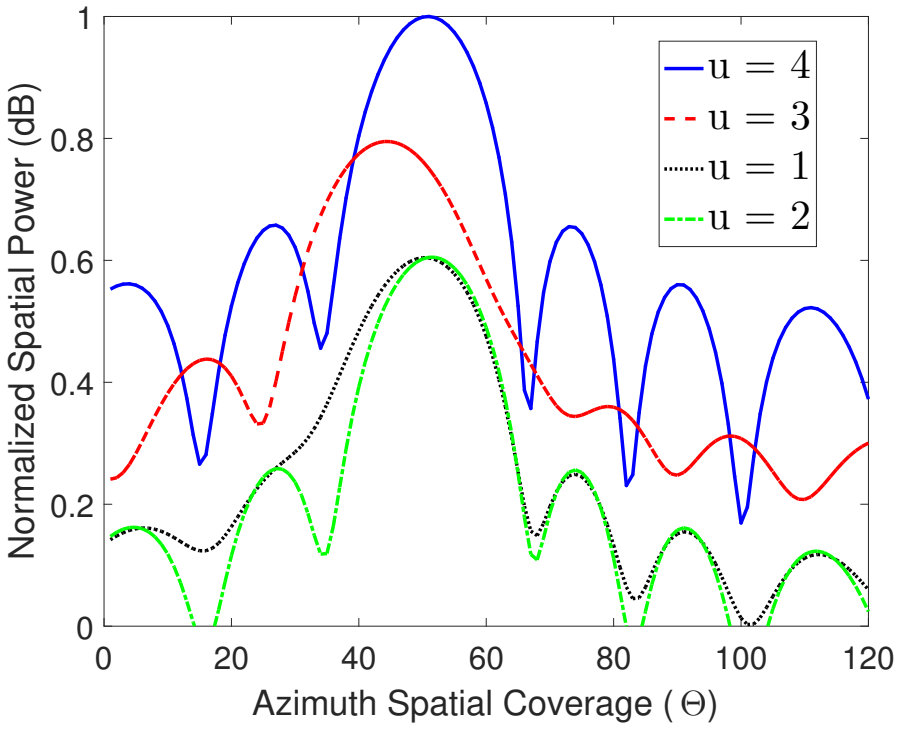

Figure 4.3: Full-dimensional UL spatial spectra.

$$\mathbf{P}_{\kappa}(\phi) = \left[a_{\kappa}^{\mathrm{H}}(\phi) \left(\mathbf{H}_{\kappa} \mathbf{H}_{\kappa}^{\mathrm{H}} \right)^{-1} a_{\kappa}(\phi) \right]^{-1}. \tag{4.12}$$

Hence, the correlation coefficient of the UL and DL clusters is calculated as

$$\rho = \frac{\int \left(\mathbf{P}_{\mathrm{ul}}(\phi) - \overline{\mathbf{P}_{\mathrm{ul}}(\phi)} \right) \left(\mathbf{P}_{\mathrm{dl}}(\phi) - \overline{\mathbf{P}_{\mathrm{dl}}(\phi)} \right) d\phi}{\sqrt{\left(\mathbf{P}_{\mathrm{ul}}(\phi) - \overline{\mathbf{P}_{\mathrm{ul}}(\phi)} \right)^2} \sqrt{\left(\mathbf{P}_{\mathrm{dl}}(\phi) - \overline{\mathbf{P}_{\mathrm{dl}}(\phi)} \right)^2}}. \tag{4.13}$$

The empirical cumulative density function (ECDF) of the correlation coefficient is shown in Figure 4.2, for different Ω values. As can be noticed, the UL and DL spatial spectra, and hence, the receive and transmit responses are highly correlated in the spatial domain, due to the small channel spatial variance over the closely-spaced antenna elements, e.g., for 50% of the channel samples, a correlation coefficient $\rho = 0.8588$ is observed for $\Omega = 200$ MHz.

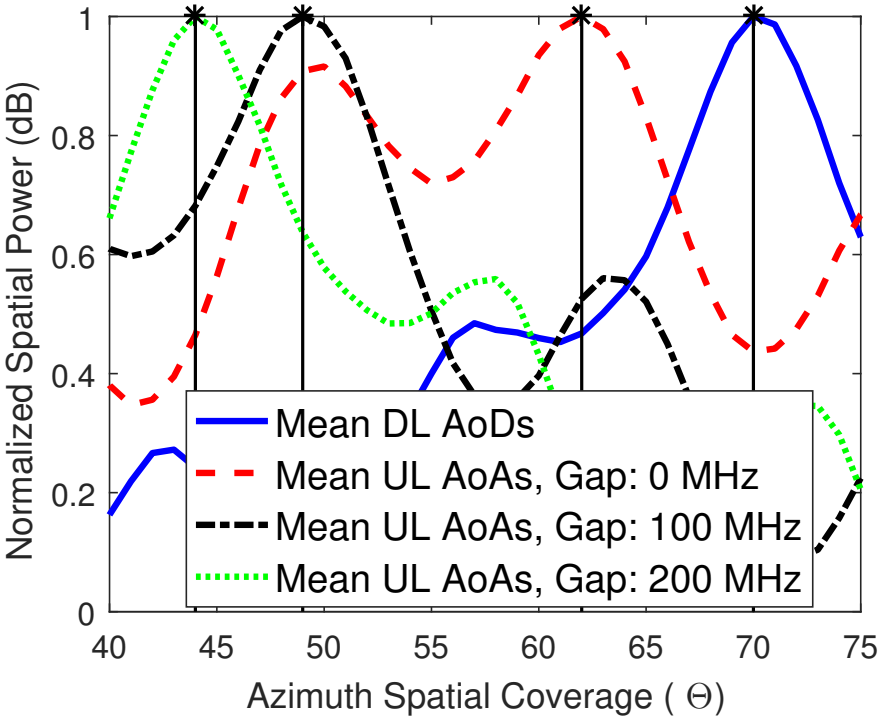

Figure 4.4: Spatial deviation of the first principal UL/ DL cluster, with Ω.

Figure 4.3 depicts the decomposable spatial spectra of the UL channel across the entire azimuthal space of each elevation subspace, with $U = 4$ and $Q = 120$. It is evident that the fourth elevation subspace ($u = 3$) is the best-match-subspace for maximizing the received signal-to-interference-noise ratio (SINR), capturing the additional UL spatial elevation DoFs. It is worth mentioning that $Q \geqslant N_t$ should be satisfied in order to fully utilize the spatial DoFs of the antenna array. Figure 4.4 exemplifies the impact of Ω on the spatial deviation between the observed UL AoAs and actual DL AoDs across the principal elevation space. It is worth noting that a spatial shift between the most dominant clusters of the UL and DL channels is noticed, as a function of Ω.

4.4.2 FD Directional Spatial Channel Estimation

The proposed D-SCE algorithm decomposes the observed UL channel into 2D projections over the azimuthal and elevation dimensions, using a pre-designed FD beamforming codebook. The principal sub-array receive responses in both dimensions are estimated to satisfy the maximization of the spatial SINR. Then, the receive responses are spatially rotated, in terms of Ω, to estimate the BS transmit responses. The observed UL channel is spatially beamformed towards the directions of the estimated transmit responses. Finally, the MMSE criterion is applied to enhance the estimation precision.

First, an arbitrary FD beamforming codeword $\mathbf{W}_\kappa(\theta, \varphi) \in \mathbb{C}^{N_t \times 1}$ is composed as

$$\mathbf{W}_\kappa(\theta, \varphi) = \frac{1}{\sqrt{N_t}} \left(\mathbf{a}_\kappa^h(\theta) \otimes \mathbf{a}_\kappa^v(\varphi) \right). \tag{4.14}$$

Accordingly, an FD beamforming spatial codebook is constructed as $\{\mathbf{W}_\kappa(\theta_q, \varphi_u)\}$, to cover the FD antenna sector by the discrete direction set $\{\theta_q, \varphi_u\}, \forall q = 0, 1, \ldots Q - 1, u = 0, 1, \ldots, U - 1$. Next, the UL FD spatial spectrum is estimated according to (12), where the array responses are substituted by the FD codewords from the codebook as $a_\kappa(\phi) = \mathbf{W}_\kappa(\theta_q, \varphi_u)$. The principal elevation subspace $\hat{\varphi_u}$ of the UL spatial spectrum is obtained based on the maximization of the average received power over the corresponding *Q-codeword* azimuthal discrete space $\{\theta_q\}$ as

$$\hat{\varphi_u} = \arg \max_{\{\varphi_u\}} \left(\mathbb{E} \left(\|\mathbf{P}_{\text{ul}}(\theta_q, \varphi_u)\|^2 \right) \right). \tag{4.15}$$

The strongest N_t azimuthal directions are estimated as

$$\hat{\theta}_n = \arg \max_{\{\theta_q\}} \left(\|\mathbf{P}_{\text{ul}}(\theta_q, \hat{\varphi_u})\|^2 \right), \forall n = 0, 1, \ldots, N_t - 1. \tag{4.16}$$

The FD array principal receive response matrix $\mathbf{A}_{\mathrm{R}}(\Theta, \hat{\varphi}_u) \in \mathbb{C}^{N_t \times N_t}$ can be given by

$$\mathbf{A}_{\mathrm{R}}(\Theta, \hat{\varphi}_u) = \left[\left(\mathbf{a}_{\mathrm{ul}}^{h}(\hat{\theta}_0) \otimes \mathbf{a}_{\mathrm{ul}}^{v}(\hat{\varphi}_u) \right)^{\mathrm{T}} \dots \left(\mathbf{a}_{\mathrm{ul}}^{h}(\hat{\theta}_{N_t-1}) \otimes \mathbf{a}_{\mathrm{ul}}^{v}(\hat{\varphi}_u) \right)^{\mathrm{T}} \right], \tag{4.17}$$

where $\Theta = \left\{ \hat{\theta}_n \right\}_{n=0}^{N_t-1}$ is the discrete set of the estimated principal azimuthal subspaces. A spatial rotation matrix $\mathbf{\Gamma} \in \mathbb{C}^{N_t \times N_t}$ is constructed to compensate for the frequency band gap between the UL and DL channels, with each rotation column vector given by

$$\digamma = \left[1, e^{-j2\pi \left(\frac{f_{dl}}{f_{ul}} \right)}, \dots, e^{-j2\pi(N_t-1) \left(\frac{f_{dl}}{f_{ul}} \right)} \right]^{\mathrm{T}}, \tag{4.18}$$

where f_{dl} and f_{ul} are the operating center frequencies of the DL and UL channels, respectively. The corresponding FD transmit response matrix $\mathbf{A}_{\mathrm{T}}(\Phi, \Psi) \in \mathbb{C}^{N_t \times N_t}$ is estimated by spatially rotating the obtained receive responses through $\mathbf{\Gamma}$ by

$$\mathbf{A}_{\mathrm{T}}(\Phi, \Psi) = \mathbf{A}_{\mathrm{R}}(\Theta, \hat{\varphi}_u) \mathbf{\Gamma}^{\mathrm{T}}, \tag{4.19}$$

where Φ and Ψ denote a rotated set of the azimuthal subspaces Θ and the elevation $\hat{\varphi}_u$ subspace. A rough estimate of the DL channel is calculated by beamforming the observed UL channel over the estimated transmit responses as: $\mathbf{H}_{\mathrm{dl}}^{(1)} = \mathbf{H}_{\mathrm{ul}}^{\mathrm{H}} \mathbf{A}_{\mathrm{T}}(\Phi, \Psi)$. Finally, the estimated transmit response matrix, is refined by applying the MMSE criterion. The MMSE approach seeks a matrix $\mathbf{G}$ to minimize the corresponding MSE as $\mathrm{MSE} = \mathbb{E}\left\{ (\mathbf{G}\mathbf{H}_{\mathrm{ul}}^{\mathrm{H}} \mathbf{A}_{\mathrm{T}}(\Phi, \Psi) - \mathbf{H}_{\mathrm{dl}})(\mathbf{G}\mathbf{H}_{\mathrm{ul}}^{\mathrm{H}} \mathbf{A}_{\mathrm{T}}(\Phi, \Psi) - \mathbf{H}_{\mathrm{dl}})^{\mathrm{H}} \right\}$; the $\mathbf{G}$ matrix is given by

$$\mathbf{G} = ((\mathbf{H}_{\mathrm{ul}}^{\mathrm{H}} \mathbf{A}_{\mathrm{T}}(\Phi, \Psi))^{\mathrm{H}} \mathbf{H}_{\mathrm{ul}}^{\mathrm{H}} \mathbf{A}_{\mathrm{T}}(\Phi, \Psi) + \sigma^2 \mathbf{I})^{-1} (\mathbf{H}_{\mathrm{ul}} \mathbf{H}_{\mathrm{ul}}^{\mathrm{H}} \mathbf{A}_{\mathrm{T}}(\Phi, \Psi)). \tag{4.20}$$

The final DL channel estimate is then expressed as

$$\mathbf{H}_{\mathrm{dl}}^{(2)} = \mathbf{H}_{\mathrm{ul}}^{\mathrm{H}} \mathbf{G} \mathbf{A}_{\mathrm{T}}(\Phi, \Psi). \tag{4.21}$$

4.5 Numerical Results

We adopt an 8×8 URA transmit antenna setup and 2×1 receive antennas. The performance of the proposed D-SCE is compared with the state-of-the-art CSIT harvesting standards for FD-mMIMO channels as follows:

Beamformed CSI-RS

The original 3GPP proposal [8] has shown significant CSIT acquisition gain. The enhanced-CSI-RS (E-CSI-RS) algorithm [9] is an extension of the CSI-RS standard, proposed from *Intel Research*. E-CSI-RS algorithm adopts dual FD-DFT codebooks. The first $L-$codeword codebook $\mathcal{J}$ defines the actual CSI-RS span, physically beamformed across the FD cell space. Thus, the beamformed DL channel $\mathbf{H}_{\mathrm{dl}}^{bf}$ at the user side is de-beamformed to obtain an approximate estimate of the actual channel $\mathbf{H}_{\mathrm{dl}}^{approx}$ span given as $\mathbf{H}_{\mathrm{dl}}^{approx} = \mathbf{H}_{\mathrm{dl}}^{bf} \mathcal{J} \mathcal{J}^{\mathrm{H}}$. At the user side, the estimate of the DL full-span channel $\mathbf{H}_{\mathrm{dl}}^{approx}$ is spatially projected over the second $N-$codeword codebook $\mathfrak{T}$. Finally, each UE feeds-back its serving BS with an index $\varkappa$ of $\mathrm{B} = \log_2(N)$ bits, to select the closest-match codeword to its estimated DL channel as $\hat{\varkappa} = \arg\max_{\mathfrak{T}} ||\mathbf{H}_{\mathrm{dl}}^{approx} \mathfrak{T}||^2$. Hence, the actual CSIT gain is L; however, the effectively harvested gain is N, where $N \gg L$.

Kronecker-based Beamforming

The KP-based CSIT approach [6] is an extension of the current 2D-MIMO CSIT standards. KP-based CSIT algorithms adopt the current double-codebooks in LTE-Pro standards [5] for the azimuthal scanning, where the azimuthal t^{th} codeword,

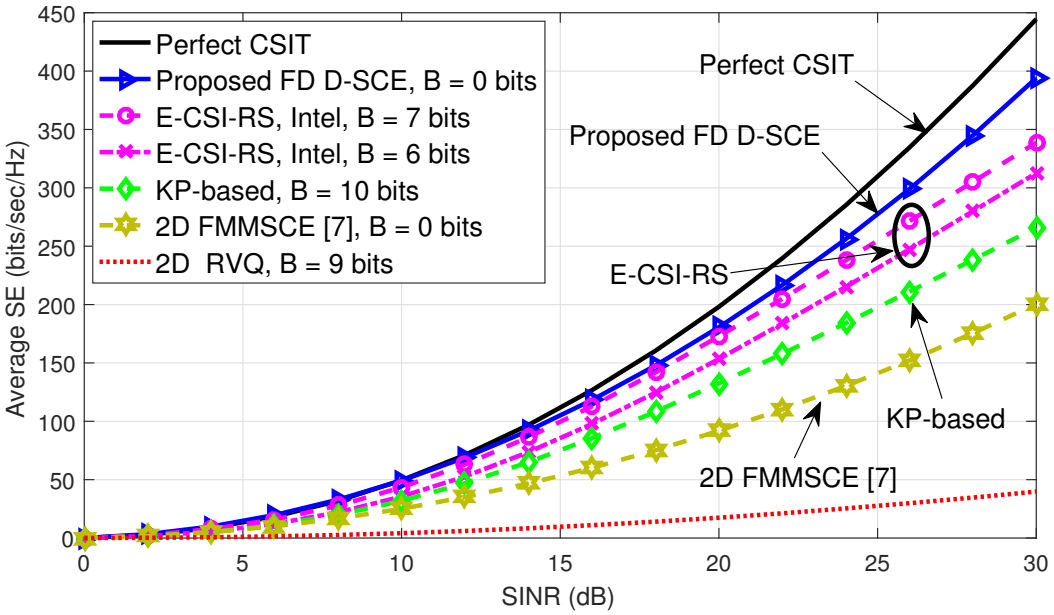

Figure 4.5: Average SE performance of the perfect CSIT, D-SCE, E-CSI-RS, KP-based CSIT, 2D FMMSCE and 2D RVQ algorithms.

for $N_h = 8$ horizontal antenna setup, is given as $(\mathcal{T})_t = \left(\frac{1}{\sqrt{8}}\right)\left[\varpi, e^{\frac{j\pi t}{2}}\varpi\right]^{\mathrm{T}}$, where $\varpi = \left[1, e^{\frac{j2\pi t}{32}}, e^{\frac{j4\pi t}{32}}, e^{\frac{j6\pi t}{32}}\right]$. For the elevation scanning, a DFT-based codebook $\mathbf{a}^{v}_{\kappa}(\varphi)$ is used, and the final FD-KP-based codebook is generated by $\mathbf{W}(\theta, \varphi) = \mathcal{T} \otimes \mathbf{a}^{v}_{\kappa}(\varphi)$.

Figure 4.5 depicts the average SE performance in bits/sec/Hz of the perfect CSIT, proposed FD D-SCE, E-CSI-RS, KP-based, 2D FMMSCE [7] and the 2D random vector quantization (RVQ) algorithms. The proposed D-SCE with B = 0 feedback overhead bits outperforms the E-CSI-RS with B = 7 bits per user per channel coherence time, especially in the high SINR region, approaching the perfect CSIT case. The E-CSI-RS suffers from performance degradation due to the channel approximation, which contributes to the residual inter-user interference. The proposed D-SCE provides significant outperformance than the KP-based CSIT with B = 10 bits, e.g., 4-elevation and 256-azimuthal codewords, respectively, due to the insufficient CSIT precision of the adopted azimuthal LTE-Pro dual-codebook. FMMSCE and conven-

tional RVQ clearly suffer from performance degradation due to the missing elevation beamforming, with B = 0 and 9 bits, respectively.

The performance gain of the proposed D-SCE algorithm is due to i) the proper reduction of the spatial channel span, and ii) the *on-the-go* sufficient estimation of the principal transmit responses. It is worth noting that a similar behavior of the D-SCE algorithm is also achieved under different antenna configurations and UL channel estimation error.

4.6 Conclusion

A novel FD directional spatial channel estimation (D-SCE) algorithm has been proposed. It blindly utilizes the statistical spatial correlation between the UL and DL channels, to attain higher CSIT harvesting gain. Compared to the state-of-the-art standard CSIT estimation algorithms, the proposed D-SCE algorithm shows significant performance improvement without FD CSIT overhead. With simple implementation complexity, zero CSIT overhead, and scalability with the size of the transmit array, the proposed D-SCE algorithm is a strong candidate for FD-mMIMO FDD

References

[1] Study on Elevation Beamforming/ Full-Dimension (FD) MIMO for LTE, 3GPP, TR 36.897, V13.0.0, June 2015.

[2] T. L. Marzetta, G. Caire, M. Debbah, I. Chih-Lin, and S. K. Mohammed, "Special issue on massive MIMO," *J. Commun. Netw.*, vol. 15, no. 4, pp. 333–337, Aug. 2013.

[3] A. A. Esswie, M. El-Absi, O. A. Dobre, S. Ikki, and T. Kaiser, "Spatial channel estimation-based FDD-MIMO interference alignment systems," *IEEE Wireless Commun. Lett.*, vol. 6, no. 2, pp. 254-257, Apr. 2017.

[4] Y. Liu, G. Y. Li, and W. Han, "Quantization and feedback of spatial covariance matrix for massive MIMO systems with cascaded precoding," *IEEE Trans. Commun.*, vol. 65, no. 4, pp. 1623-1634, Apr. 2017.

[5] Downlink Multiple Input Multiple Output (MIMO) enhancement for LTE-Advanced, 3GPP, TR 36.871, Dec. 2011.

[6] 2D Codebook with KP structure and associated feedback, Ericsson, 3GPP TSG-RAN, WG1 MEETING #81: R1-153168, May 2015.

[7] A. A. Esswie, M. El-Absi, O. A. Dobre, S. Ikki, and T. Kaiser, "A novel FDD massive MIMO system based on downlink spatial channel estimation without CSIT," in *Proc. IEEE ICC*, Paris, 2017, pp. 1-6.

[8] Precoding Schemes for Elevation Beamforming/ FD-MIMO, NTT Docomo, 3GPP, TSG-RAN, WG1 MEETING #80: R1-151983, Apr. 2015.

[9] G. Morozov, A. Davydov, and V. Sergeev, "Enhanced CSI feedback for FD-MIMO with beamformed CSI-RS in LTE-A Pro systems," in *Proc. IEEE VTC-Fall*, Montreal, 2016, pp. 1-5.

[10] Study on 3D Channel Model for LTE, 3GPP, TR 36.873, Sep. 2014.

Chapter 5

Conclusion

In this chapter, the conclusions drawn by the dissertation are presented. The potential extensions are additionally introduced for future development.

5.1 Conclusion

- Practical channels are not spatially uncorrelated, which in turn leads to invalidating the widely-used assumption of the independent and identically distributed (i.i.d) Rayleigh channel modeling. The i.i.d channel modeling facilitates deriving closed-form rate expressions for multi-antenna communications. However, practical channels are demonstrated of being spatially correlated through field measurements campaigns, where the UL and DL channel clusters have correlated arrival and departure directions, respectively. Thus, a standard spatial channel model is introduced in wireless standards to reflect the practical channel considerations, which is adopted allover this dissertation.

- Interference is a major limitation of the cellular communications. Strong interference leads to significant loss in the network spectral efficiency, capacity,

and coverage. In the recent literature, interference mitigation has been a key focus towards the next generation cellular networks. The interference alignment transmission technique is considered a strong candidate for future cellular networks because it achieves the optimal network capacity with limited interference levels. However, interference alignment requires perfect CSIT, which leads to severe feedback overhead in the uplink direction, e.g., 20/30 bits per user per channel coherence time.

- In Chapter 3, we proposed a spatial channel estimation for MIMO interference alignment systems. The proposed algorithm utilizes the spatial correlation between the UL and DL channels, to find an approximate estimate of the downlink channel. It combines both the proper estimation accuracy and the effective beamforming gain to provide significant performance improvement, approaching the ideal case. It is shown that the proposed algorithm relieves the interference alignment systems from the requirements of the channel quantization and user feedback.

- In Chapter 4, we extend our system model to the mMIMO model, where large antenna arrays are employed at the base-station. mMIMO systems provide great spatial DoFs which allows simple linear interference mitigation techniques to fully control the inter-user interference, without the need for complex transmission strategies. However, channel quantization and feedback are considered fundamental limitations against mMIMO systems, because the feedback overhead is shown to scale linearly with the number of transmit antennas. Our proposed algorithm shows scalability with the size of the transmit antenna array, while providing significant performance improvement. Without complex processing or user feedback overhead, the mMIMO systems with our proposed

algorithm can be a strong transmission candidate for future wireless networks.

- Finally, we extend the dimensionality of the proposed algorithm to the full dimensional space, where more realistic user distributions are considered. In practical dense deployments, user distributions can not be controlled, where users may be distributed across sparse elevation and azimuthal directions. Current standards consider beamforming only the azimuthal direction, to reduce the size of the user feedback overhead only to the azimuthal direction. However, this leads to suboptimal performance when the user location does not align with the bore-sight of the beamforming direction. The recent full dimensional beamforming standards require significant feedback overhead from each user, which is non-feasible in practice. We proposed a blind estimation algorithm for full dimensional beamforming, where no user feedback overhead or channel quantization are needed. Compared to the state-of-the-art full dimensional beamforming standards, the proposed algorithm shows promising performance enhancement while preserving the practical limitations such as the constant modulus, and the fixed alphabet.

5.2 Future Research Directions

The acquisition of the CSIT for interference alignment and 2D/3D mMIMO systems is still in its infant phase of developments; hence, there are couple of suggested directions to extend the work in this dissertation as follows:

- Extension to multi-cell communications may be worth investigation, by considering the inter-cell interference. For interference alignment transmissions, base-stations must collaborate to design the joint precoders for the cell edge users. The coordination overhead and structure may be further investigated.

- Deriving an optimal closed-form expression for the rotation parameter is shown to be a hard problem, because the estimation problem is non-convex and varies with several factors such as the antenna array structure, the frequency band gap, channel model, and user conditions. The proposed algorithms, under all considered setups, compensate for the most impacting factor: the frequency band gap; however, this approximation is not optimal. A further investigation with other impacting parameters would be of an interest.

Chapter 6

References

Chapter 1

[1] "Global Mobile Data Traffic Forecast Update, 2015 – 2020", CISCO, 2017.

[2] M. Ptzold, "5G developments are in full swing [Mobile Radio]," *IEEE Veh. Technol. Mag.*, vol. 12, no. 2, pp. 4-12, June 2017.

[3] C. Yang, J. Li, Q. Ni, A. Anpalagan and M. Guizani, "Interference-aware energy efficiency maximization in 5G ultra-dense networks," *IEEE Trans. Commun.*, vol. 65, no. 2, pp. 728-739, Feb. 2017.

[4] S. Hamid, A. J. Al-Dweik, M. Mirahmadi, K. Mubarak and A. Shami, "Inside-out propagation: developing a unified model for the interference in 5G networks," *IEEE Veh. Technol. Mag.*, vol. 10, no. 2, pp. 47-54, June 2015.

[5] T. Y. Wu and T. Chang, "interference reduction by millimeter wave technology for 5G-based green communications," *IEEE Access*, vol. 4, pp. 10228-10234, 2016.

[6] X. Jiang, M. Čirkić, F. Kaltenberger, E. G. Larsson, L. Deneire and R. Knopp, "MIMO-TDD reciprocity under hardware imbalances: Experimental results," *in Proc. IEEE ICC*, London, 2015, pp. 4949-4953.

[7] A. A. Esswie, M. El-Absi, O. A. Dobre, S. Ikki and T. Kaiser, "Spatial channel estimation-based FDD-MIMO interference alignment systems," *IEEE Commun. Lett.*, vol. 6, no. 2, pp. 254-257, April 2017.

[8] Y. Han, W. Shin and J. Lee, "Projection-based differential feedback for FDD massive MIMO systems," *IEEE Trans. Veh. Technol.*, vol. 66, no. 1, pp. 202-212, Jan. 2017.

[9] J. Song, J. Choi, K. Lee, T. Kim, J. y. Seol and D. J. Love, "Advanced quantizer designs for FD-MIMO systems using uniform planar arrays," *in Proc. IEEE GLOBECOM*, Washington, DC, 2016, pp. 1-6.

[10] Ali A. Esswie, Mohammed El-Absi, Octavia A. Dobre, Salama Ikki and Thomas Kaiser, “A novel FDD massive MIMO system based on downlink spatial channel estimation without CSIT,” in *Proc. IEEE ICC*, Paris, 2017, pp. 1-6.

[11] Ali A. Esswie, Octavia A. Dobre, and Salama Ikki, “Directional spatial channel estimation for massive FD-MIMO in next generation 5G networks,” *to be submitted.*

[12] T. L. Marzetta, G. Caire, M. Debbah, I. Chih-Lin, and S. K. Mohammed, “Special issue on massive MIMO,” *J. Commun. Netw.*, vol. 15, no. 4, pp. 333–337, 2013.

[13] Study on 3D channel model for LTE,” 3GPP, TR 36.873, Sep. 2014.

[14] L. Berriche, K. Abed-Meraim, and J.-C. Belfiore, "Investigation of the channel estimation error on MIMO system performance," *in Proc. EUSIPCO*, Antalya, Turkey, Sep. 2005, pp. 1–4.

[15] T. Marzetta, "How much training is required for multi user MIMO?" *in Proc. ACSSC*, Oct. 2006, pp. 359–363.

[16] J. Hoydis et al., "Massive MIMO in the UL/DL of cellular networks: How many antennas do we need?" *IEEE J. Sel. Areas Commun.*, vol. 31, no. 2, pp. 160–171, Feb. 2013

[17] J. Jose, A. Ashikhmin, T. Marzetta, and S. Vishwanath, "Pilot contamination and precoding in multi-cell TDD systems," *IEEE Trans. Wireless Commun.*, vol. 10, no. 8, pp. 2640–2651, Aug. 2011

[18] T. Marzetta and B. Hochwald, "Fast transfer of channel state information in wireless systems," *IEEE Trans. Signal Process.*, vol. 54, no. 4, pp. 1268–1278, Apr. 2006

[19] Y. Yu and D. Gu, "Enhanced MU-MIMO downlink transmission in the FDD-based distributed antennas system," *IEEE Commun. Lett.*, vol. 16, no. 1, pp. 37–39, Jan. 2012.

[20] J. Chang, I. Lu, and Y. Li, "Adaptive codebook-based channel prediction and interpolation for multiuser multiple-input multiple-output orthogonal frequency division multiplexing systems," *IET Commun.*, vol. 6, no. 3, pp. 281–288, Feb. 2012.

[21] A. Rajanna and N. Jindal, "Multiuser diversity in downlink channels: When does the feedback cost outweigh the spectral efficiency benefit?" *IEEE Trans. Wireless Commun.*, vol. 11, no. 1, pp. 408–418, Jan. 2012.

[22] G. Taricco and E. Biglieri, “Space-time decoding with imperfect channel estimation,” *IEEE Trans. Wireless Commun.*, vol. 4, no. 4, pp. 1874– 1888, Jul. 2005

[23] T. Shuang, T. Koivisto, H. L. Maattanen, K. Pietikainen, T. Roman and M. Enescu, "Design and Evaluation of LTE-Advanced Double Codebook," *in Proc. VTC*, Yokohama, 2011, pp. 1-5.

[24] L. Tong, B. M. Sadler, and M. Dong, “Pilot-assisted wireless transmissions: general model, design criteria, and signal processing,” *IEEE Signal Process. Mag.*, vol. 21, no. 6, pp. 12–25, Nov. 2004

[25] M. Coldrey and P. Bohlin, “Training based MIMO systems—Part I : Performance comparison,” *IEEE Trans. Signal Process.*, vol. 55, no. 11, pp. 5464–5476, Nov. 2007.

[26] M. Coldrey and P. Bohlin, “Training Based MIMO systems—Part II: improvements using detected symbol information,” *IEEE Trans. Signal Process.*, vol. 56, no. 1, pp. 296–303, Jan. 2008.

[27] Y. Xie, S. Jin, J. Wang, Y. Zhu, X. Gao, and Y. Huang, “A limited feedback scheme for 3D multiuser MIMO based on kronecker product codebook,” *in Proc. IEEE PIRMC*, London, 2013, pp. 1130-1135..

[28] D. Yang, L.-L. Yang, and L. Hanzo, “DFT-based beamforming weight-vector codebook design for spatially correlated channels in the unitary precoding aided multiuser downlink,” *in Proc. IEEE Int. Communi. Conf.*, 2010

[29] Y. Song, S. Nagata, H. Jiang and L. Chen, "CSI-RS design for 3D MIMO in future LTE-advanced," *in Proc. ICC*, Sydney, NSW, 2014, pp. 5101-5106.

[30] Precoding Schemes for Elevation Beamforming and FD-MIMO, NTT DOCOMO, 3GPP, TSG RAN WG1, MEETING # 80: R1-151983, 2015.

[31] A. Esswie and A. Fouda, "Three-dimensional progressive rotated codebook for advanced multi-user MIMO in LTE-A networks," *in Proc. ATC*, Ho Chi Minh City, 2015, pp. 20-25.

[32] M. Sajadieh, A. Esswie, A. Fouda, H. Shirani-Mehr and D. Chatterjee, "Progressive channel state information for advanced multi-user MIMO in next generation cellular systems," *in Proc. WCNC*, Doha, 2016, pp. 1-6.

[33] M. Narandzic, C. Schneider, R. Thoma, T. Jamsa, P. Kyosti and X. Zhao, "Comparison of SCM, SCME, and WINNER Channel Models,"*in Proc. VTC-Spring*, Dublin, 2007, pp. 413-417.

[34] B. Clerckx, G. Kim, and S. Kim, "Correlated fading in broadcast MIMO channels: Curse or blessing?" *in Proc. IEEE GLOBECOM*, New Orleans, LO, 2008, pp. 1-5.

[35] A. Adhikary, J. Nam, J.-Y. Ahn, and G. Caire, "Joint spatial division and multiplexing the large-scale array regime," *IEEE Trans. Inform. Theory,* vol. 59, no. 10, pp. 6441–6463, Oct. 2013.

[36] H. Abut, Vector quantization, 1st ed. New York: IEEE Press, 1990.

[37] V. Raghavan, R. W. Heath Jr., and A. M. Sayeed, "Systematic codebook designs for quantized beamforming in correlated MIMO channels," *IEEE J. Select. Areas Commun.*, vol. 25, no. 7, pp. 1298–1310, Sep. 2007.

[38] Y. Huang, L. Yang, M. Bengtsson, and B. Ottersten, “Exploiting long-term channel correlation in limited feedback SDMA through channel phase codebook,” *IEEE Trans. Signal Process.*, vol. 59, no. 3, pp. 1217–1228, Mar. 2011.

[39] J. Choi, V. Raghavan, and D. J. Love, “Limited feedback design for the spatially correlated multi-antenna broadcast channel,” *in Proc. IEEE GLOBECOM*„ Atlanta, GA, 2013, pp. 3481-3486.

Chapter 2

[1] M. El-Absi, “Novel Aspects of Interference Alignment in Wireless Communications,” PhD. thesis, Duisburg-Essen Univ., Germany, 2015.

[2] N. Zhao, F. R. Yu, M. Jin, Q. Yan, and V. C. M. Leung, "Interference Alignment and Its Applications”, Research Issues, and Challenges," *IEEE Commun. Soc. Mag.*, vol. 18, no. 3, pp. 1779-1803, Mar. 2016.

[3] V. R. Cadambe, S. A. Jafar, and S. Shamai, "Interference Alignment on the Deterministic Channel and Application to Fully Connected Gaussian Interference Networks," *IEEE Trans. Inform. Theory.*, vol. 55, no. 1, pp. 269-274, Jan. 2009.

[4] X. Rao and V. K. N. Lau, "Minimization of CSI Feedback Dimension for Interference Alignment in MIMO Interference Multicast Networks," *IEEE Trans. Inform. Theory.*, vol. 61, no. 3, pp. 1218-1246, Mar. 2015.

[5] A. Jafar, *Interference Alignment — A New Look at Signal Dimensions in a Communication Network*. Boston: Foundations and Trends in Communications and Information Theory, 2011.

[6] O. El Ayach and R. W. Heath, "Grassmannian Differential Limited Feedback for Interference Alignment," *IEEE Trans. Signal Process.*, vol. 60, no. 12, pp. 6481-6494, Apr. 2012.

[7] S. M. Razavi and T. Ratnarajah, "Performance Analysis of Interference Alignment Under CSI Mismatch," *IEEE Trans. Veh. Technol.*, vol. 63, no. 9, pp. 4740-4748, Nov. 2014.

[8] H. Huang, V. Lau, Y. Du, and S. Liu, "Robust Lattice Alignment for MIMO Interference Channels With Imperfect Channel Knowledge," *IEEE Trans. Signal Process.*, vol. 59, no. 7, pp. 3315-3325, July 2011.

[9] M. Rezaee and M. Guillaud, "Limited Feedback for Interference Alignment in the K-user MIMO Interference Channel," in *Proc. IEEE ITW*, Lausanne, 2012, pp. 667-671

[10] M. Kim, H. Lee, and Y. Ko, "Limited Feedback Design for Interference Alignment on Two-Cell Interfering MIMO-MAC," *IEEE Trans. Veh. Technol.*, vol. 64, no. 9, pp. 4019-4030, Sep. 2015.

[11] Spatial Channel Model for Multiple Input Multiple Output (MIMO) Simulations (Release 11), 3GPP, TR 25.996 V11.0.0, Sep. 2012.

[12] H. Xie, F. Gao, S. Zhang, and S. Jin, "A Unified Transmission Strategy for massive MIMO Systems with Spatial Basis Expansion Model," *IEEE Trans. Veh. Technol.*, vol. PP, no. 99, pp. 1-14, Mar. 2016.

Chapter 3

[1] T. L. Marzetta, “Noncooperative Cellular Wireless With Unlimited Numbers of Base Station Antennas,” *IEEE Trans. Wireless Commun.*, vol. 9, no. 11, pp. 3590–3600, Nov. 2010.

[2] T. L. Narasimhan and A. Chockalingam, "Channel Hardening-Exploiting Message Passing Receiver in Large-Scale MIMO Systems," *IEEE J. Sel. Topics Signal Process.*, vol. 8, no. 5, pp. 847-860, Oct. 2014.

[3] M. El-Absi, M. El-Hadidy, and T. Kaiser, “A Distributed Interference Alignment Algorithm Using Min-Maxing Strategy,” *Trans. Emerging Telecommun. Technol.*, Oct. 2014.

[4] A. Afana, T. M. N. Ngatched and O. A. Dobre, "Spatial Modulation in MIMO Limited-Feedback Spectrum-Sharing Systems With Mutual Interference and Channel Estimation Errors," *IEEE Commun. Lett.*, vol. 19, no. 10, pp. 1754-1757, Oct. 2015.

[5] D. J. Love, R. W. Heath Jr., V. K. N. Lau, D. Gesbert, B. D. Rao, and M. Andrews., “An Overview Of Limited Feedback In Wireless Communication Systems,” *IEEE J. Sel. Area Commun.*, vol. 26, no. 8, pp. 1341-1365, Oct. 2008.

[6] E. Bjornson, J. Hoydis, M. Kountouris, and M. Debbah, “Massive MIMO Systems With Non-Ideal Hardware: Energy Efficiency, Estimation, and Capacity limits,” *IEEE Trans. Inf. Theory*, vol. 60, no. 11, pp. 7112-7139, Nov. 2014.

[7] C. Shepard, H. Yu, N. Anand, L. E. Li, T. L. Marzetta, R. Yang, and L. Zhong, “Argos: Practical Many-Antenna Base Stations,” *in Proc. ACM Mobicom Netw. Conf.*, 2012, pp. 53-64.

[8] A. Decurninge, M. Guillaud, and D. Slock, “Channel Covariance Estimation In massive MIMO Frequency Division Duplex Systems,” *in Proc. IEEE GLOBECOM*, San Diego, CA, 2015, pp. 1-6.

[9] A. Adhikary, J. Nam, J.-Y. Ahn, and G. Caire, “Joint Spatial Division and Multiplexing: The Large-Scale Array Regime,” *IEEE Trans. Inf. Theory*, vol. 59, no. 10, pp. 6441–6463, Oct. 2013.

[10] M. Sajadieh, A. Esswie, A. Fouda, H. Shirani-Mehr and D. Chatterjee, "Progressive Channel State Information For Advanced Multi-User MIMO In Next Generation Cellular Systems," *in Proc. IEEE WCNC*, Doha, 2016, pp. 1-6.

[11] H. Xie, F. Gao, S. Zhang and S. Jin, "A Unified Transmission Strategy for massive MIMO Systems with Spatial Basis Expansion Model," *IEEE Trans. Veh. Technol.*, vol. PP, no. 99, pp. 1-14, Mar. 2016.

[12] H. Wang, W. Wang, V. K. N. Lau, and Z. Zhang, "Hybrid Limited Feedback in 5G Cellular Systems With massive MIMO," *IEEE Systems Journal*, vol. PP, no. 99, pp. 1-12, Aug. 2015.

[13] Spatial Channel Model for Multiple Input Multiple Output (MIMO) Simulations (Release 11), 3GPP, TR 25.996 V11.0.0, Sep. 2012.

[14] A. Esswie, M. El-Absi, O. A. Dobre, S. Ikki, and T. Kaiser, “Spatial Channel Estimation Based FDD-MIMO Interference Alignment Systems,” *Accepted in IEEE Wireless Commun. Lett.*, Feb. 2017.

[15] C. K. Au-Yeung and D. J. Love, “On The Performance of Random Vector Quantization Limited Feedback Beamforming In a MISO System,” *IEEE Trans. Wireless Commun.*, vol. 6, no. 2, pp. 458-462, Feb. 2007.

[16] G. Caire and S. Shamai, “On The Achievable Throughput of a Multi-Antenna Gaussian Broadcast Channel,” *IEEE Trans. Inf. Theory*, vol. 49, no. 7, pp. 1691-1706, Jul. 2003

[17] Evolved Universal Terrestrial Radio Access (E-UTRA); Physical layer procedures (Release 12), 3GPP, TS 36.213 V12.4.0, Feb. 2015.

[18] S. Faxer, S. Bergman, and N. Wernersson, "A Codebook-Based Concept for Hybrid CSI Feedback in FDD massive MIMO Systems," *in Proc. IEEE VTC Spring*, 2016, pp. 1-6.

[19] X. Rao and V. K. Lau, “Distributed Compressive CSIT Estimation and Feedback For FDD Multi-User massive MIMO Systems,” *IEEE Trans. Signal Process.*, vol. 62, no. 12, pp. 3261–3271, June 2014.

Chapter 4

[1] Study on Elevation Beamforming/ Full-Dimension (FD) MIMO for LTE, 3GPP, TR 36.897, V13.0.0, June 2015.

[2] T. L. Marzetta, G. Caire, M. Debbah, I. Chih-Lin, and S. K. Mohammed, “Special issue on massive MIMO,” *J. Commun. Netw.*, vol. 15, no. 4, pp. 333–337, Aug. 2013.

[3] A. Esswie, M. El-Absi, O. A. Dobre, S. Ikki, and T. Kaiser, “Spatial channel estimation based FDD-MIMO interference alignment systems,” *IEEE Wireless Commun. Lett.*, Feb. 2017.

[4] Y. Liu, G. Y. Li and W. Han, "Quantization and feedback of spatial covariance matrix for massive MIMO systems with cascaded precoding," *IEEE Trans. Commun.*, vol. 65, no. 4, pp. 1623-1634, April 2017.

[5] Downlink Multiple Input Multiple Output (MIMO) enhancement for LTE-Advanced, 3GPP, TR 36.871, Dec. 2011.

[6] 2D Codebook with KP structure and associated feedback, Ericsson, 3GPP TSG-RAN, WG1 MEETING #81: R1-153168, May 2015.

[7] Ali A. Esswie, Mohammed El-Absi, Octavia A. Dobre, Salama Ikki and Thomas Kaiser, “A novel FDD massive MIMO system based on downlink spatial channel estimation without CSIT,” in *Proc. IEEE ICC*, Paris, 2017, pp. 1-6.

[8] Precoding Schemes for Elevation Beamforming/ FD-MIMO, NTT Docomo, 3GPP, TSG-RAN, WG1 MEETING #80: R1-151983, April 2015.

[9] G. Morozov, A. Davydov and V. Sergeev, "Enhanced CSI Feedback for FD-MIMO with Beamformed CSI-RS in LTE-A Pro Systems," in *Proc. IEEE VTC-Fall*, Montreal, QC, 2016, pp. 1-5.

[10] Study on 3D Channel Model for LTE, 3GPP, TR 36.873, Sep. 2014.